(51) International Patent Classification 6 : G03F 7/20	A1	(11) International Publication Number: WO 98/32054
		(43) International Publication Date: 23 July 1998 (23.07.98)

(54) Title: METHODS AND APPARATUS FOR INTEGRATING OPTICAL AND INTERFEROMETRIC LITHOGRAPHY TO PRODUCE COMPLEX PATTERNS

(57) Abstract

The present invention provides methods and apparatus for defining a single structure (11) on a semiconductor wafer by spatial frequency components whereby some of the spatial frequency components (12–16) are derived by optical lithography and some by interferometric lithography techniques. Interferometric lithography images the high frequency components while optical lithography images the low frequency components. Optics collects many spatial frequencies and the interferometry shifts the spatial frequencies to high spatial frequencies. Thus, because the mask does not need to provide high spatial frequencies, the masks are configured to create only low frequency components, thereby allowing fabrication of simpler masks having larger structures. These methods and apparatus facilitate writing more complex repetitive as well as non–repetitive patterns in a single exposure with a resolution which is higher than that currently available using known optical lithography alone.

METHODS AND APPARATUS FOR INTEGRATING
OPTICAL AND INTERFEROMETRIC LITHOGRAPHY
TO PRODUCE COMPLEX PATTERNS

Inventors: S.R.J. Brueck, Xiaolan Chen, Andrew Frauenglass, and Saleem H. Zaidi

5   *Technical Field*

The present invention relates, generally, to the use of interferometric techniques to produce repetitive structures during semiconductor fabrication and, more particularly, to the integration of interferometric lithography with optical lithography to produce arbitrarily complex patterns on wafers.

10   *Background Art and Technical Problems*

Progress in the production of integrated circuits employing very large scale integration (VLSI) has been characterized by an ever decreasing feature size. Transverse dimensions of transistor features have decreased from ~5 micrometers in 1970 (4K DRAM) to 0.35 micrometers today (64M DRAM). This continuous improvement in
15   feature size is an integral part of "Moore's Law", which projects an exponential feature size decrease characterized by a reduction of 30% in linear dimensions every three years. This "law" underlies the semiconductor industry planning as exemplified in the "National Technology Roadmap for Semiconductors" (Semiconductor Industry Association, 1994), incorporated herein by this reference.

20   Throughout this progress, optical lithography has remained the dominant lithographic technique for manufacturing applications. Many advances have been made in optical lithography to allow this dramatic scale reduction. The optical wavelength used in state-of-the-art lithographic tools has decreased from mercury G-line (436 nm) to mercury I-line (365 nm) to 248 DUV (KrF laser). Currently, 193 nm ArF laser-based
25   steppers are being developed, continuing this historical trend. At the same time optical systems have been improved from numerical apertures (*NA*) of 0.2 to ~0.6-0.7.

There are several factors which together suggest that additional major improvements along these directions are not likely, and that the industry will have to undergo a significant change in lithographic technique. Chief among these factors is the
30   reduction of the feature size to below the available optical wavelengths. Additionally, there is an increasing premium on line width control for high-speed circuit operation,

even as the scale reduction below the wavelength is making line width control more
difficult. For wavelengths below the 193 nm ArF wavelength, transmitting optical
materials are believed to be unavailable, and a transition to an all-reflective system will
likely be required. This is problematical since current multi-layer reflector and aspheric

5   optical technologies are not sufficiently developed to meet these needs. Most likely, the
transition to reflective optics will result in a significant reduction in the possible *NAs*,
reducing the benefit of shorter wavelengths.

Optical sources with sufficient average power for high throughput manufacturing
are another major problem for wavelengths shorter than 193 nm. EUV lithography is a

10   promising approach based on a laser-produced plasma source and 5X reduction, aspheric,
all-reflective optics with multi layer reflectors. However, it is not yet clear whether this
program will lead to a cost effective lithography tool that can timely meet the needs of
the industry for the next generation lithographic capability.

A further factor suggesting a substantial change in lithographic techniques

15   surrounds the complexity of the masks required for future ULSI generations. This
complexity is, by definition, increasing by a factor of four each generation (*i.e.*, four
times as many transistors on a chip). In addition, many of the potential solutions to the
optical lithography problem, collectively known as resolution-enhancement techniques,
lead to increased mask complexity (*e.g.*, with the introduction of serifs, helper bars, and

20   other sub-resolution features) or require a three-dimensional mask in place of the
traditional chrome-on-glass two-dimensional masks (phase shift techniques). These
trends are increasing the difficulty and cost of producing ULSI structures at high yields.

A number of alternative lithographic technologies are being investigated. These
include: X-ray, e-beam, ion-beam and probe-tip technologies. Each of these has its

25   advantages and disadvantages, but it is safe to state that none of them has as yet emerged
as a satisfactory alternative to optical lithography.

Interferometric lithography, *i.e.*, the use of the standing wave pattern produced by
two or more coherent optical beams to expose a photoresist layer, has recently been
demonstrated to provide a very simple technique to produce the requisite scale for the

30   next several ULSI generations. *See, for example*, U.S. Patent No. 5,415,835, issued May
16, 1995, to Steven R.J. Brueck, Saleem Zaidi and An-Shyang Chu, entitled *Fine-Line
Interferometric Lithography*; U.S. Patent No. 5,216,257, issued June 1, 1993, to Steven
R.J. Brueck and Saleem H. Zaidi, entitled *Overlay of Submicron Lithographic Features*;

U.S. Patent No. 5,343,292, issued August 30, 1994, to Steven R.J.Brueck and Saleem H. Zaidi, entitled *Method and Apparatus for Alignment of Submicron Lithographic Features*; U.S. Patent Application SN 07/662,676, filed February 2, 1991, by Kenneth P. Bishop, Steven R.J. Brueck, Susan M. Gaspar, Kirt C. Hickman, John R. McNeil, S.

5   Sohail H. Naqvi, Brian R. Stallard and Gary D. Tipton, entitled *Use of Diffracted Light from Latent Images in Photoresist for Exposure Control*; U.S. Patent Application SN 08/399,381, filed February 24, 1995, by Steven R.J. Brueck, Xiaolan Chen, Saleem Zaidi and Daniel J. Devine, entitled Methods and Apparatuses for *Lithography of Sparse Arrays of Sub-Micrometer Features* _____, filed _____, by S.R.J. Brueck,

10   An-Shiang Chu, Saleem Zaidi, and Bruce L. Draper, entitled *Method for Fabrication of Quantum Wires and Quantum Dots and Arrays of Same*; U.S. Patent No. 5,247,601, issued September 21, 1993, to Richard A. Myers, Nandini Mukherjee and Steven R.J. Brueck, entitled *Arrangement for Producing Large Second-Order Optical Nonlinearities in a Waveguide Structure Including Amorphous SIO2*; U.S. Patent No. 5,239,407, issued

15   August 24, 1993, to Steven R.J. Brueck, Richard A. Myers, Anadi Muskerjee and Adam Wu, entitled *Methods and Apparatus for Large Second-Order Nonlinearities in Fused Silica;* U.S. Patent No. 4,987,461, issued January 22, 1991, to Steven R.J. Brueck, S. Schubert, Kristin McArdle and Bill W. Mullins, entitled *High Position Resolution Sensor with Rectifying Contacts*; U.S. Patent No. 4,881,236, issued November 14, 1989, to

20   Steven R.J. Brueck, Christian F. Schauss, Marek A. Osinski, John G. McInerney, M. Yasin A. Raja, Thomas M. Brennan and Burrell E. Hammons, entitled *Wavelength-Resonant Surface-Emitting Semiconductor Laser;* U.S. Patent Application SN 08/635,565, filed September 16, 1992, by Steven R.J. Brueck, Saleem Zaidi and An-Shyang Chu, entitled *Method for Fine-Line Interferometric Lithography;* U.S. CIP Patent

25   Application SN 08/407,067, filed March 16, 1995, by Steven R.J. Brueck, Xiaolan Chen, Saleem Zaidi and Daniel J. Devine, entitled *Methods and Apparatus for Lithography of Sparse Arrays of Sub-Micrometer Features;* U.S. Patent Application SN 08/123,543, filed September 20, 1993, by Steven R.J. Brueck, An-Shyang Chu, Bruce L. Draper and Saleem H. Zaidi, entitled *Method for Manufacture of Quantum Sized Periodic Structures*

30   *in Si Materials;* U.S. FWC Patent Application SN 08/490,101, filed June 6, 1995, by Steven R.J. Brueck, An-Shyang Chu, Bruce L. Draper and Saleem Zaidi, entitled *Method for Manufacture of Quantum Sized Periodic Structures in Si Materials;* U.S. DIV Patent Application SN 08/719,896, filed September 25, 1996, by Steven R.J. Brueck, An-

Shyang Chu, Bruce L. Draper and Saleem H. Zaidi, entitled *Manufacture of Quantum Sized Periodic Structures in Si Materials*; U.S. Patent Application SN 07/847,618, filed March 5, 1992, by Kenneth P. Bishop, Lisa M. Milner, S. Sohail H. Naqvi, John R. McNeil and Bruce L. Draper, entitled *Use of Diffracted Light from Latent Images in* 5 *Photoresist for Optimizing Image Contrast;* U.S. Patent Application SN 08/525,960, filed September 8, 1995, by Steven R.J. Brueck and Xiang-Cun Long, entitled *Technique for Fabrication of a Poled Electrooptic Fiber Segment;* U.S. Patent No. 5,426,498, filed June 20, 1995, by Steven R.J. Brueck, David B. Burckel, Andrew Frauenglass and Saleem Zaidi, entitled *Method and Apparatus for Real-time* Speckle *Interferometry for Strain or* 10 *Displacement of an Object Surface;* SIA, *National Technology Roadmap for Semiconductors* (1994); J.W. Goodman, *Introduction to Fourier Optics*, 2nd Ed. (McGraw Hill, NY 1996); J.W. Goodman, *Statistical Optics* (John Wiley, NY 1985); Xiaolan Chen, S.H. Zaidi, S.R.J. Brueck and D.J. Devine, *Interferometric Lithography of Sub-Micrometer Sparse Hole Arrays for Field-Emission Display Applications* (Jour. 15 Vac. Sci. Tech B14, 3339-3349, 1996); S.H. Zaidi and S.R.J. Brueck, *Multiple-Exposure Interferometric Lithography* (Jour. Vac. Sci. Tech. B11, 658, 1992); A. Yariv, *Introduction to Optical Electronics* (Holt, Reinhard and Winston, NY 1971). The entire contents of the foregoing are hereby incorporate herein by this reference.

The limiting spatial frequency in interferometric lithography is generally regarded 20 as ~$\lambda/2$, where λ is the laser wavelength, and the critical dimension (CD) for 1:1 lines and spaces is $\lambda/4$. This should be contrasted with the limiting CD of imaging optical systems which is usually stated as $k_1\lambda/NA$, where k_1 is a function of manufacturing tolerances as well as of the optical system, λ Is the center wavelength of the exposure system, and NA is the numerical aperture of the imaging optical system. Typical values 25 of k_1 range from 1.0 down to ~0.6. This is an oversimplified description of the limiting scales, but serves to illustrate the major points. Projections for the 193 wavelength optical lithography tool are an NA of 0.6 which leads to a limiting CD of ~0.19 micrometer. In contrast, at I-line (365 nm) interferometric lithography has a limiting resolution of ~0.09 micrometer. Using the 193 wavelength, the limiting resolution of 30 interferometric lithography is ~0.05 micrometer. This is already better than the current projections for EUV lithography (a wavelength of 13 nm and a NA of 0.1 leading to a CD of 0.08 micrometer at a k_1 of 0.6).

- 4 -

A major obstacle associated with interferometric lithography surrounds the development of sufficient pattern flexibility to produce useful circuit patterns in the VLSI and ULSI context. A two-beam interferometric exposure simply produces a periodic pattern of lines and spaces over the entire field. Multiple beam (4 or 5) exposures produce two-dimensional structures, but also of relatively simple repeating patterns such as holes or posts. More complex structures can be made by using multiple interferometric exposures, for example as described in U.S. Patent No. 5,415,835, issued May 16, 1995, to S.R.J. Brueck and Saleem H. Zaidi, entitled *Method and Apparatus for Fine-Line Interferometric Lithography* and in Jour. Vac. Sci. Tech. B11 658 (1992). Additional flexibility may be attained by combining interferometric and optical lithography as also described in the above patent. Thus far, demonstrations include relatively simple examples, *e.g.*, defining an array of lines by interferometric lithography and delimiting the field by a second optical exposure. Multiple exposures have been demonstrated to produce more complex, but still repetitive structures.

In addition to limited pattern flexibility, presently known interferometric lithography techniques lack a well-defined synthesis procedure for obtaining a desired structure.

A technique is thus needed which overcomes, *inter alia*, the foregoing drawbacks associated with prior art techniques.

Summary of the Invention

The present invention provides methods and apparatus for integrating optical lithography and interferometric lithography in a manner which overcomes many of the shortcomings of the prior art.

A preferred embodiment of the present invention provides methods and apparatus for parsing the lithographic tasks between optical and interferometric lithographic techniques. In accordance with a particularly preferred embodiment, an optical system is provided which facilitates the integration of interferometric lithography and optical lithography to produce complex structures on the same workpiece, for example a semiconductor wafer. In a preferred exemplary embodiment, two masks are configured to intercept two portions of a uniform, collimated optical beam which is imaged by the optical system onto the wafer. An interferometric optical system is incorporated into the apparatus to bring the two mask images onto the wafer at substantially equal and opposite

angles with respect to a wafer normal plane. In accordance with this preferred embodiment, the masks are suitably tilted relative to the optical axis in order to produce image planes which are coincident with the wafer plane after passing through the interferometric optics.

5   In accordance with a further aspect of the present invention, a formal parsing procedure is proposed for separating an arbitrary desired pattern into a number of specified interferometric and optical lithography exposures.

In accordance with a further aspect of the present invention, multiple beam interferometric lithography is extended to include a number of discrete spatial frequencies

10   or, alternatively, a continuous range of spatial frequencies, to thereby facilitate writing more complex repetitive as well as non-repetitive patterns in a single exposure.

In accordance with a further aspect of the present invention. methods and apparatus are provided for combining extended multiple beam interferometric lithography with optical lithography to produce arbitrary structures at a resolution which is higher than that

15   currently available using known optical lithography alone.

In accordance with a further aspect of the present invention, methods and apparatus are provided for optically defining the masks employed in interferometric exposures.

In accordance with yet a further aspect of the present invention. methods and apparatus are provided for reducing the complexity of masks used in the optical

20   lithography portion of a combined optical and interferometric lithography exposure.

Brief Description of the Drawing Figures

The present invention will hereinafter be described in conjunction with the appended drawing figures, wherein like designations denote like elements, and:

Figure 1 is a schematic representation of the decomposition of a specific structure

25   into rectangles for facilitating a Fourier transform. with the rectangles shown slightly offset for clarity;

Figure 2 is an exemplary graph of optical transfer functions for coherent and incoherent illumination;

Figure 3 are graphical examples of prior art VLSI patterns at a 0.18 micrometers

30   CD written by diffraction-limited optical lithography tools at prescribed wavelengths and NAs; the left-hand column represents the results of incoherent illumination. and the right-hand column sets forth the results of coherent illumination;

Figure 4 illustrates examples of VLSI patterns at a 0.18 micrometer CD written using a combination of optical and interferometric exposures;

Figure 5 sets forth a simplification of the mask structure in the context of integrated optical and interferometric lithographic techniques;

Figure 6 is a schematic representation of an exemplary optical system useful in imaging a field stop onto a wafer in accordance with a preferred embodiment of the present invention;

Figure 7 is a schematic representation of the optical system of Figure 6, extended to include interferometric lithographic techniques;

Figures 8A and 8B are schematic representations of alternate interferometric optical systems useful in producing mask images biased to high spatial frequencies;

Figures 9A and 9B depict, respectively, in-focus and out-of-focus SEM micrographs of the edge regions of a rectangular aperture imaged using the optical system of Figure 8A;

Figure 10 is a schematic diagram representing the spatial frequency space representation of the combination of imaging optical and interferometric exposures;

Figure 11 is a schematic representation of an optical system for biasing the spatial frequency content of an image away from the zero center frequency in accordance with a preferred embodiment of the present invention:

Figure 12 is a schematic representation of an optical system for imaging a sub-mask using a mask of the full pattern along with a prism to bias the frequency components away from low frequency; and

Figure 13 sets forth schematic examples of VLSI patterns at 0.18 micrometer CD written at a wavelength of 365 nm by a combination of interferometric lithography using the arrangement of Figure 11, and imaging optical lithography (IIL).

Detailed Description Of Preferred Exemplary Embodiments

Before describing the subject invention in detail, a review of Fourier optics is presented. *See also,* J.W. Goodman, *Introduction to Fourier Optics,* 2nd Ed. (John Wiley Press, NY 1996), the entire contents of which are hereby incorporated herein by this reference.

For simplicity, the ensuing discussion assumes the use of incoherent illumination, so that each Fourier component of the image can be treated and evaluated independently.

The discussion will then be extended to the limit of coherent illumination where each component refers to the electric field and the result squared to determine the intensity at the exposure plane. In practice, actual optical lithography tools typically employ partially coherent illumination. For a more detailed discussion of partial coherence, *see, for example,* J.W. Goodman, *Statistical Optics* (John Wiley, NY 1985). Although the use of partially coherent illumination adds to the computational complexity of the mathematical analysis, it does otherwise significantly impact the present invention as set forth herein.

An optical lithography system can be separated into an illumination subsystem, a mask, the imaging optical subsystem, and the photoresist optical response. The purpose of the illumination subsystem is to provide uniform illumination of the mask. On passing through the mask, the optical beam is diffracted into a number of plane waves corresponding to the Fourier components of the mask pattern. Each of these plane wave components propagates in a different spatial direction, characterized by the k_x and k_y components of the wavevector. Mathematically, this is described in the plane of the mask as:

$$(1) \qquad f(x,y) = \sum_{k_x}\sum_{k_y} F(k_x,k_y)e^{i2\pi(k_x x + k_y y)}$$

where the summations run over the allowed spatial frequencies, $k_x = n/P_x$; $n = 0, \pm1, \pm2,$ ...; $k_y = m/P_y$; $m = 0, \pm1, \pm2,$ ..., and P_x and Py are the repeat periods of the pattern in the x and y directions, respectively. P_x and P_y can be as large as the exposure die size for a non-repeating pattern. Since a chrome-on-glass mask has a binary transmission function (each pixel is either unity or zero), the Fourier transform in (1) is just given by a sum over $\sin(x)/x$ functions with appropriate phase shifts corresponding to a decomposition of the desired pattern into rectangles. That is:

$$(2) \qquad F(k_x,k_y) = \sum_i a_i b_i \frac{\sin(2\pi k_x a_i/2)}{2\pi k_x a_i/2} \frac{\sin(2\pi k_y b_i/2)}{2\pi k_y b_i/2} e^{i2\pi(k_x c_i + k_y d_i)}$$

where a_i (b_i) is the extent of each rectangle in x (y), and c_i (d_i) is the offset of the rectangle center from the coordinate origin in x (y).

With momentary reference to **Figure 1**, the foregoing decomposition of the desired pattern into rectangles is illustrated schematically for a typical VLSI gate structure. In

- 8 -

particular, an exemplary pattern, shown in the illustrated embodiment as a typical gate 11, is decomposed into a plurality of rectangles 12-16, shown offset in the **Figure** for clarity.

The imaging optical subsystem imposes a modulation transfer function (MTF) on the propagation of the Fourier components onto the image (wafer) plane. For diffraction limited optics with circular symmetry, the transfer function is characterized by a spatial frequency, $k_{opt} = NA/\lambda$ where NA is the numerical aperture and λ the center wavelength. In the limit of incoherent illumination, the MTF is given by *see* Goodman, *Introduction to Fourier Optics*, 2nd Ed. (McGraw Hill, NY 1996):

$$(3) \qquad T_{incoh}(k_x, k_y) = \left\{ \frac{2}{\pi} \left[\cos^{-1}\left(\frac{k}{2k_{opt}}\right) - \frac{k}{2k_{opt}} \sqrt{1 - \left(\frac{k}{2k_{opt}}\right)^2} \right] \right\} \text{ for } k \leq 2k_{opt}$$

where $k = \sqrt{k_x^2 + k_y^2}$; and $T_{incoh}(k_x, k_y) = 0$ for $k > 2k_{opt}$. For a coherent optical system, the transfer function is simply

$$(4) \qquad T_{coh}(k_x, k_y) = 1 \text{ for } k \leq k_{opt}, \text{ and } T_{coh}(k_x, k_y) = 0 \text{ for } k > k_{opt},$$

where, as noted above, this transfer function is suitably applied to the optical electric fields before evaluating the aerial image intensity.

Referring now to **Figure 2**, these two transfer functions are shown along with the transfer function for interferometric lithography that will be discussed in more detail below. The scale is set by $k_{opt} = NA/\lambda$ where NA is the optical subsystem numerical aperture and λ is the center wavelength of the illumination system. For incoherent illumination, the transfer function, T_{incoh}, is applied to each Fourier component of the intensity pattern at the mask. For coherent illumination, the transfer function, T_{incoh}, is applied to each Fourier component of the intensity pattern at the mask. For coherent illumination, the transfer function, T_{incoh}, is applied to the Fourier components of the electric field at the mask and the intensity is evaluated at the wafer plane. Also shown is the optical transfer function for interferometric lithography (23) that extends to $2/\lambda$. The parameters used to plot the **Figure** are $\lambda = 365$ nm and $NA = 0.65$. The graph of

- 9 -

Figure 2 is drawn for a *NA* of 0.6; the normalization to k/k_{opt} removes any explicit dependence on λ.

Finally, the image intensity at the wafer plane is transferred to the resist, which typically exhibits a nonlinear response. In this regard, both positive and negative tone resists are commonly used in the industry. For the sake of definiteness, the calculations presented herein are for negative tone resist (*i.e.*, illuminated regions of the resist are retained on developing, non-illuminated regions are removed). It will be understood that the calculations could equally be made to apply to a positive tone resist with a simple inversion of the mask to reverse the illuminated and non-illuminated regions. For simplicity of calculation, the photoresist response will be approximated as a step function. That is, for local intensities below a threshold value the photoresist is assumed to be fully cleared upon development, while for local intensities above the threshold value, the resist thickness is unaffected by the development process. In practice, the resist has a finite contrast and non-local intensities impact the development. The impact of these realistic considerations is to remove some of the high spatial frequency variations in the results presented below, and to yield finite sidewall slopes rather than the abrupt sidewalls predicted by this simple model. However, these effects do not impact the scope or content of the subject invention.

Referring now to **Figure 3**, an example of prior art techniques shows the results of applying this analysis to the printing of a typical VLSI gate pattern at a 0.18 micrometer CD with optical lithography tools at 365, 248 and 193 nm (bottom to top, respectively). The desired pattern is shown as the dotted lines in each cell. Only the perimeters of the patterns printed by the optical tools are shown. Inside of these perimeters the resist is exposed and remains intact on developing; outside of the perimeters the resist is unexposed and is removed during development (negative resist). As noted above, it is a simple modification to the analysis to reverse this response for positive resist. The patterns are periodic; hence, in an actual exposure, each cell would be repeated many times and, of course, the frames delineating each cell would not be printed. To provide more information in the **Figure**, adjacent cells are shown with the results of different exposure tools and illumination conditions. The *NA*s were set at 0.65 for the 365 nm (I-line) tool and at 0.6 for the 248 nm (KrF laser source) and 193 nm (ArF laser source). The left column shows the results for incoherent illumination, the right column for coherent illumination. As expected from the simple analysis presented in the background

- 10 -

section, an I-line optical lithography tool is not capable of conveniently writing a 0.18 micrometer CD structure (*e.g.*, minimum resolution of $\sim k_1\lambda/NA \sim 0.8 \times .365/.65 \sim 0.45$ micrometer). The printed shapes show severe distortions resulting from the limited frequency components available; indeed, the coherent illumination image is not even two

5   separated features but merges into a single structure. Although not shown in **Figure 3,** the patterns are also very sensitive to process variations, showing large changes for small variations in optical exposure levels. The patterns available from a 248 nm optical tool are significantly improved; however, they still show significant rounding of the edges and deviations from the desired structure. Even the patterns available from a 193 nm tool are

10   far from ideal.

The foregoing procedure can be used to parse the lithographic task between optical and interferometric lithographies. This parsing technique is at the heart of the subject invention.

Before illustrating the subject parsing techniques in detail, an evaluation of the

15   MTF for interferometric lithography is first presented.

More particularly, in its simplest form IL uses two coherent optical beams incident on the substrate with equal and opposite azimuthal angles *(q)* in a plane normal to the wafer. The intensity at the wafer is given by

$$(5) \qquad\qquad I_{IL}(x) = 2I_0 \left[1 + \cos(4\pi k \sin(\theta)x + \varphi) \right]$$

20   where the intensity of each beam individually is I_0, $k = 1/\lambda$ with λ the wavelength of the coherent beam and the phase factor *j* describes the position of the pattern with respect to the wafer coordinate system. It may be necessary to adjust this phase factor appropriately in multiple exposures (*i.e.*, inter-exposure alignment) in order to form the desired final pattern. This is a MTF of unity, *i.e.*, the intensity goes to zero at the minima. The spatial

25   frequency is given by

$$(6) \qquad\qquad k_x = 2k\sin(\theta)$$

and the maximum spatial frequency is $k_x|_{max} \equiv k_{IL} = 2/\lambda$. This should be compared with the maximum spatial frequency for an imaging optical system, viz. $k|_{max} = k_{opt} = 2NA/\lambda$. Further, the modulation transfer function for an interferometric exposure is typically unity

for all $k < k_{IL}$, in contrast to the sharp drop-off for a traditional optical system. This is illustrated in **Figure 2** along with the corresponding MTFs for both coherent and incoherent illumination optical imaging systems. It is important to remember that the MTF for coherent illumination is applied to the Fourier components of the electric field

5   rather than of the intensity. The nonlinear squaring operation involved in taking the intensity produces frequency components extending out to 2 x k_{opt}.

Thus a defined procedure for exposing a desired pattern in accordance with the present invention surrounds optical and interferometric lithographies. In accordance with a particularly preferred embodiment, the optical lithography is primarily used for the

10   lower frequency components, and the interferometric lithography is primarily used to provide the higher spatial frequency components. Thresholds can be set on the interferometric exposures both in frequency (*i.e.*, a maximum and a minimum spatial frequency) and in amplitude (eliminating any frequency components whose Fourier amplitude is below a preset level). This is illustrated in **Figure 4** for the same VLSI

15   pattern used in the prior art example (**Figure 3**).

With continued reference to **Figure 4**, the left hand column shows examples of setting frequency limits. For the top left panel, the entire frequency space available by interferometric lithography is used and, hence, there is no need for an optical lithography step in this case. The resulting pattern is a closer representation of the desired pattern that

20   any of the prior art examples, even those at substantially shorter wavelengths; however, 51 exposures were required in this example. The lower two panels in the left column show examples of restricting first the low frequencies, and then both low and high frequencies. In each case the low frequency components are driven from an optical exposure. The right hand column shows the results of setting a threshold on the intensity

25   of interferometric lithography exposures. Progressively higher thresholds (top to bottom) yield progressively fewer interferometric lithography exposures and progressively less ideal approximations to the desired structure. This phenomenon underscores the tradeoff between the number of exposures, which relates to manufacturing cost in terms of exposure time, and the pattern fidelity. This tradeoff may be advantageously optimized

30   within each level's specific context in accordance with the teachings of the present invention.

As noted above, one of the major difficulties facing optical lithography is the increasing complexity of the required masks. Since the parsing procedure outlined herein

advantageously exploits optical lithography for the low spatial frequency components of the image and supplies the high spatial frequency components by interferometric lithography, the mask complexity can be dramatically reduced.

Referring now to **Figure 5**, an exemplary VLSI pattern similar that shown in **Figure 4** is again shown using the foregoing paradigm, namely, wherein optical lithography is leveraged for the low spatial frequency components and interferometric lithography is employed for the high spatial frequency components of the mask. More particularly, the top left panel of **Figure 5** shows the image resulting from printing (incoherent imaging) only the low spatial frequency components (up to $k_{opt} = NA/\lambda$) using the full mask structure (shown as the dotted lines). The top right panel shows the results of adding 51 interferometric exposures (solid lines) (*see* **Figure 4** top left panel) and on restricting the interferometric lithography to only seven exposures with a simple amplitude threshold (dashed lines). These results are substantially equivalent to those shown in **Figure 4**. The middle left panel of **Figure 5** shows a much simpler mask (labeled simplified mask A and shown as a dotted line) and the resulting intensity profile when the image from this mask is passed through the imaging system with no restriction on spatial frequency beyond that inherent in the imaging system. This is a much simpler mask than the full pattern, but it produces very similar results within the restricted frequency space of the optical tool. Mask pattern A was derived by simple trial and error from the low frequency results in the panel above by passing the A pattern through the imaging simulation described in the preceding paragraphs. Note that because of the repetitive patterning, pattern A is simply a single rectangular aperture per reperition unit.

With continued reference to **Figure 5**, the middle right panel shows the results of using simplified pattern A for the optical exposure and adding interferometric lithography exposures (no threshold, full range of available spatial frequencies) is very close to that for the full mask. The dashed curve is for seven interferometric lithography exposures. The low frequency mask can be simplified even further to the simple straight line segment shown in the bottom left panel. Because of the repetitive pattern, this is just a wide line extending the full height of the die.

The bottom right panel of **Figure 5** shows the results of adding high frequency components using 51 (solid) and 7 (dashed) interferometric lithography exposures. The results are very close to those obtained with the full mask and are again much better than

those available even from a 193 nm optical exposure tool. There is very little difference between the resulting exposures showing that a simplified mask can be used for the optical lithography step, easing the mask making difficulty, while still retaining good pattern fidelity.   As above, a careful tradeoff between number of exposures

5   (manufacturing throughput) and pattern fidelity needs to be made for individual levels.

It is also possible to reduce the number of interferometric exposures by combining multiple (more than two) beams in a single exposure. A simple example of this is discussed at some length in related U.S. Patent Application SN 08/399,381, filed February 24, 1995, by Steven R.J. Brueck, Xiaolan Chen, Saleem Zaidi and Daniel J.

10   Devine, entitled Methods and Apparatuses for *Lithography of Sparse Arrays of Sub-Micrometer Feature*. This earlier application provides a series of techniques for writing a particular two-dimensional exposure, specifically a sparse array (> 1:3 hole diameter:interhole distance) of holes in a positive photoresist layer. Specific examples of three, four and five beam exposures are provided therein.

15   It is often desirable, and often necessary, to delimit the field of an interferometric lithography exposure. Typical die sizes (today on the order of 20×30 mm^2) for single exposures are much smaller than wafer sizes (200 mm to 300 mm diameter). In order to obtain a uniform exposure over the die, the optical beam is expanded and transformed into a uniform intensity across the field size. However, the edges of the beam are

20   necessarily nonuniform and if allowed to expose the wafer would result in a substantial pattern nonuniformity. One technique to address this is simply to add a field stop aperture just above the wafer to delimit the exposed area. A significant problem with this approach, however, surrounds the diffraction effects of the aperture. From diffraction theory, these extend ~ 10 $\sqrt{IL}$ into the pattern where L is the distance from the field stop

25   to the wafer. For a practical separation distance of L ~ *1 mm*, this diffraction ringing extends ~ 0.3 mm into the pattern. In many applications, this is an unacceptable result. One technique for eliminating this ringing is to make the aperture rough on the scale of the wavelength, so that fields scattered from the edge to not add coherently away from the edge.

30   Another alternative, more in keeping with traditionally lithography and providing significantly enhanced flexibility, is to move the field stop away from the wafer and add an optical system that provides two functions simultaneously: 1) image the field stop onto

- 14 -

the wafer, and 2) transform the collimated beam incident onto the field stop into a collimated beam at the wafer.

Referring now to **Figure 6**, a preferred exemplary embodiment of an optical system used to image a field stop 31 onto a wafer 32 comprises respective lenses 33 and 34 having focal lengths f_1 and f_2 where the mask 31 is placed a distance f_1 before first lens 33, wherein the separation between the lenses is suitably $f_1 + f_2$, and the wafer 32 is placed a distance f_2 behind second lens 34. The magnification of the image is given by $-f_1/f_2$. The field stop is suitably disposed before the first lens 33 and illuminated by a laser source that is collimated (*i.e.*, the wavefront has a very large radius of curvature) and approximately uniform across the area of the field stop. In this configuration, the curvature of the wavefront is substantially unaffected by this optical system. The diffraction-limited edge definition of the field stop image at the wafer is suitably proportional to the wavelength and inversely proportional to the numerical aperture of the optical system. This is only one of a class of optical systems that serve to transfer both the mask image and at the same time retain the overall wavefront flatness. The general condition specifying suitable optical systems is that the B and C terms of the overall ABCD ray transfer matrix describing the optical system be zero. (*cf.* A. Yariv, *Introduction to Optical Electronics* (Holt, Reinhart and Winston, NY 1971), for a discussion of ABCD ray-tracing transfer matrices).

The mathematical description of this imaging system is straightforward in terms of the Fourier optics concepts introduced above. Since the mask illumination is with a coherent uniform beam, a coherent imaging analysis is appropriate. The electric field just after the mask can be written as:

$$E_{mask}(x,y) = \sum_{k_x}\sum_{k_y} M(k_x,k_y) e^{i2\pi k_x x} e^{i2\pi k_y y}$$

(7)

where $M(k_x, k_y)$ is the Fourier transform of the mask transmission function and for convenience is assumed discrete. For an aperiodic mask pattern, the summations over k_x, k_y are replaced by integrals in the usual fashion. Passing through the optical system imposes a modulation transfer function:

$$T_E(k_x,k_y) = 1 \quad for \quad \sqrt{k_x^2 + k_y^2} < k_{opt} \equiv NA/\lambda$$
$$= 0 \quad for \quad \sqrt{k_x^2 + k_y^2} > k_{opt}$$

(8)

where the E subscript is a reminder that this transfer function is applied to the electric field rather than the intensity. Then the electric field at the wafer is given by:

(9)

$$E_{mask}(x,y) = \sum_{k_x}\sum_{k_y} M(k_x,k_y)T_E(k_x,k_y)e^{i2\pi k_x x}e^{i2\pi k_y y}$$

and the intensity is given by

5   (10)

$$I_{wafer}(x,y) = \left| E_{wafer}(x,y) \right|^2$$

$$= \sum_{k_x'}\sum_{k_x''}\sum_{k_y'}\sum_{k_y''} M(k_x',k_y')T_E(k_x',k_y')M(k_x'',k_y'')T_E(k_x'',k_y'')e^{i2\pi(k_x'+k_x'')x}e^{i2\pi(k_y'+k_y'')y}$$

$$= \sum_{k_x'}\sum_{k_y'} I(k_x',k_y')e^{2\pi i k_x' x}e^{2\pi i k_y' y}$$

where λ is the Fourier transform of the intensity, real for a simple transmission mask, and the primes on k_x ', and k_y ' indicate that, as a result of the squaring operation, they are composed of appropriate sums of the k_x and k_y of the electric field Fourier transform and extend out to $2x k_{opt}$.

10   The low frequency pattern defined by the mask can be shifted to higher spatial frequencies by splitting the optical path and introducing interferometric optics. Referring now to **Figure 7**, a preferred exemplary embodiment of the present invention illustrates the optical system of **Figure 6** extended to include apparatus for integrating interferometric techniques into the lithography system. More particularly, respective

15   masks 41 and 42, which are not necessarily identical, are suitably introduced into two portions (*e.g.*. halves) of the optical beam, shown on the figure as upper and lower. In order to compensate for any tilt introduced into the phase front by the final optical elements, these masks may be advantageously placed at a tilt so that the final image plane is in the wafer normal. The optical system consists of lenses 33 and 34 positioned as

20   described in reference to **Figure 6** . Finally, interferometric optics are introduced in order to provide the high frequency bias.

The interferometric optical system shown in **Figure 7** suitably comprises a plurality (*e.g.*, four) of mirrors (45, 46, 47 and 48) that split the optical beam into respective segments (*e.g.*, two) and cause these segments to interfere at the plane of wafer 15. In the illustrated embodiment, the interferometric optical system is suitably configured to bring the mask images onto the wafer at substantially equal and opposite angles to the wafer normal. The advantages of this system include equal center path lengths for the two beams and an absence of induced astigmatism.

Referring now to **Figure 8**, various alternate embodiments may be employed to produce mask images biased to high spatial frequencies. In particular, **Figure 8A** employs a simple Fresnel configuration comprising a Fresnel lens 23 and a mirror 51 configured to apply the mask image to the workpiece (*e.g.*, wafer) 32. Although the configuration of **Figure 8A** is attractive in that it is a much simpler configuration involving only one mirror (51), the two center path lengths are unequal, requiring different mask planes for the two masks. **Figure 8B** shows a prism (52) configuration, where the center path lengths are equal, but the prism introduces an astigmatism requiring different mask planes for x-lines and y-lines.

The mathematical description of these systems will now be derived in terms of **Figure 7**. Small changes that do not affect the essential results are required to adapt this description to the alternate optical schemes of **Figure 8**. Adapting Equation 9 to the optical system of **Figure 7** gives:

$$
E_{wafer}(x,y) = \left[\sum_{k_x}\sum_{k_y} M_u(k_x,k_y)T_E(k_x,k_y)e^{i2\pi k_x x}e^{i2\pi k_y y} \right]e^{i2\pi wx}
$$

(11)

$$
+ \left[\sum_{k_x}\sum_{k_y} M_l(k_x,k_y)T_E(k_x,k_y)e^{i2\pi k_x x}e^{i2\pi k_y y} \right]e^{-i2\pi wx}
$$

where subscripts u, λ have been added to the mask Fourier transforms to indicate that they are

not necessarily identical; $w=2p\sin q/\lambda$ is the spatial frequency bias added to each beam by the interferometric optics. Taking the intensity gives the image printed on the photoresist layer, *viz.*:

$$
I_{wafer}(x,y) = \left| E_{wafer}(x,y) \right|^2 = \sum_{k_x}\sum_{k_y} I_u(k_x',k_y')e^{i2\pi k_x' x}e^{i2\pi k_y' y} + \sum_{k_x}\sum_{k_y} I_l(k_x',k_y')e^{i2\pi k_x' x}e^{i2\pi k_y' y}
$$

(12)

$$
+2\sqrt{\sum_{k_x}\sum_{k_y} I_u(k_x',k_y')e^{i2\pi k_x' x}e^{i2\pi k_y' y} \sum_{k_x}\sum_{k_y} I_l(k_x',k_y')e^{i2\pi k_x' x}e^{i2\pi k_y' y}} \cos(4\pi wx)
$$

- 17 -

and in the special case that the two masks are identical this reduces to:

$$(13) \qquad I_{wafer}(x,y) = 2\sum_{k_x}\sum_{k_y} 1(k_x', k_y')e^{i2\pi k_x'x}e^{i2\pi k_y'y}\left[1+\cos(4\pi wx)\right]$$

Equation (13) corresponds to the mask image modulated by the high frequency interferometric pattern. For example, if the mask pattern is simply a field stop, then the resulting printed pattern will be a high spatial frequency line:space pattern, delimited at the edges by the field stop. As noted above, the edge of the field stop is typically defined to within a distance of $\sim \lambda/NA$ by the limitations of the optical system. More complex mask patterns are clearly possible; indeed any mask pattern within the spatial frequency limits of the optical system can be reproduced with the additional, high-spatial-frequency modulation introduced by the interferometric optical system in accordance with the present invention.

Referring now to **Figure 9**, a plurality of SEM micrographs are presented illustrating an initial experimental demonstration using the optical arrangement of **Figure 8A** to print a uniform line:space pattern within a finite field. The optical source was a Ar-ion laser at 364 nm. This was a very low NA optical system (~ 0.06), using only single-element, uncorrected, spherical lenses, so that the diffraction limited edge definition was only ~ 6 mm and there is probably a significant contribution from lens aberrations. The top two SEMs **(Figure 9A)** show the in-focus case. Both the vertical edge of the field stop (parallel to the interferometric grating lines) and the horizontal edge (perpendicular to the interferometric grating lines) are defined to within ~ 10 mm. This edge definition is within a factor of 2 to 3 of the theoretical diffraction limit ($\lambda/NA\sim4$ mm). Notice that the grating period of 0.9 mm essentially provides a built-in measuring apparatus. In contrast, the bottom SEMs **(Figure 9B)** show similar results for an out-of-focus condition. The intensity fringing at the edges is due to diffraction; the distance to the first fringe of ~ 30 mm can be used to calibrate the distance from the focal plane (*i.e.*, the defocus) at about 3.5 mm.

Equation 13 can be rewritten to emphasize the distribution of spatial frequency contributions associated with this image. *viz.*:

$$I_{wafer}(x,y) = 2\sum_{k_x}\sum_{k_y} I(k_x',k_y')e^{i2\pi k_x'x}e^{i2\pi k_y'y}[1+\cos(4\pi wx)]$$

(14)
$$= 2\sum_{k_x}\sum_{k_y} I(k_x',k_y')e^{i2\pi k_x'x}e^{i2\pi k_y'y} + \sum_{k_x}\sum_{k_y} I(k_x',k_y')e^{i2\pi k_x'x}e^{i2\pi k_y'y}\left[e^{i2\pi(2w+k_x')x}+e^{-i2\pi(2w-k_x')x}\right]$$

Close scrutiny of Equation (14) suggests that there are three regions of frequency space with significant frequency content: the low frequency region modified by the lens system and represented by the intensity term, and two replicas of this intensity pattern, one

5   shifted by $+2wx$ and one by $-2wx$ as a result of the interferometric optics. This situation is illustrated in **Figure 10A** which suitably models the full extent of frequency space covered by the exposure described in Equation 14 using an exemplary optical system such as that shown in **Figure 8A**. In particular, the full extent of available frequency space is modeled as the large circle 104 with radius $k_{ll} = 2/\lambda$, with the three filled-in

10   circles 106, 108, and 110 representing the aforementioned three regions of frequency space with significant frequency content. For the optical system used in the demonstration of **Figure 9**, the low frequency region is contained within a circle of radius $2k_{opt} = 2NA/\lambda$, with $NA = 0.06$, and the two interferometrically created regions are offset by $2w = 2\sin(q)/\lambda$ and $\sin(q) = 0.2$ for a 0.9 mm pitch grating. The radius of each offset region is

15   equal to that of the low frequency region. From Equation 3, the MTF of the optical system decreases monotonically along a radial direction in each of these frequency regions and is zero at the edges of the circles depicted in **Figure 10A**. Note that the lens optical system alone (**Figure 6**) is incapable of creating the 0.9 mm period grating, whereas the interferometric system combined with the lens system (**Figure 8A**) has

20   shifted the frequency content of the image to the higher frequencies necessary to produce the grating while retaining the low frequency content that defines the area of the image. Importantly, the combined optical system results in an image whose frequency content covers continuous regions of frequency space; this should be contrasted to the discussion of periodic structures above in which only points in frequency space, relatively widely

25   separated for the small period pattern ($12\times CD$ in x, $5\times CD$ in y) are needed to reproduce the pattern (*see, for example*, the above discussion of **Figures 1, 3, 4 and 5**).

For this first demonstration, a very modest optical system was used. As is clear from **Figure 10A**, the resulting pattern covers only a very small region of the available frequency space. **Figure 10B** shows the possibility of covering much of spatial frequency

30   space with a small number of exposures and a modest optical system, *e.g.*, for a lens NA of 0.33. Offset regions in frequency space are shown in both the k_x- and k_y-directions.

These could be provided in two exposures using optical systems analogous to those shown in **Figures 7 and 8**, or in a single exposure with a four-beam interferometric system as is discussed for the plane wave case (*e.g.*, single points in frequency space) in U.S. Patent Application SN 08/399,381, filed February 24, 1995, by Steven R.J. Brueck,

5   Xiaolan Chen, Saleem Zaidi and Daniel J. Devine, entitled *Methods and Apparatuses for Lithography of Sparse Arrays of Sub-Micrometer Features*. Because the relative phases of the frequency components along the k_x- and k_y-axes may vary from pattern to pattern, it is likely that two exposures will be required. The *NA* of $\lambda/3$ was chosen since this is the smallest *NA* for which, along a diameter between three circles, continuous coverage of

10   frequency space is achieved. Since the frequency response of the optical system is inadequate at the edges of the circles, either additional exposures or a larger *NA* optical system are required to achieve full coverage. Rectilinear patterns have the majority of their frequency content concentrated close to the k_x- and k_y-axes; so that this frequency space coverage may be satisfactory. If not, additional exposures, or additional beam

15   paths, or both may be employed, as desired.

Even with sufficient exposures at a large enough *NA* to assure complete coverage of frequency space, this arrangement does not conveniently permit the imaging of arbitrary patterns. This is because each intensity pattern represents a real mask image; this places some constraints on the Fourier components. Specifically, for a simple

20   transmission mask described by Equation 10 the requirement that the intensity after the mask is real and positive requires

$$I(k_x, k_y) = I^*(-k_x, -k_y)$$

(15)

This same relationship must hold for the final image. However, the interferometric optical system imposes a more constraining relationship, *e. g.*

25   (16)
$$
\begin{aligned}
I(k_x, k_y) &= I^*(-k_x, -k_y) \\
&= I(k_x + 2w, k_y) = I^*(-k_x - 2w, -k_y) \\
&= I(k_x - 2w, k_y) = I^*(-k_x + 2w, -k_y)
\end{aligned}
$$

- 20 -

Again, for the final image, the pairwise relationships shown on each line must hold, but the requirement that the relationships hold between these pairs overly constrains the final image.

In accordance with the present invention, there are at least three approaches solutions to reconciling the foregoing constraints: (1) overlap multiple exposures to break this symmetry; (2) use phase masks or other three-dimensional masks to break the overall symmetry described by Equation 15; and (3) modify the optical system by using different masks in the upper and lower arms and by introducing additional optics to shift the center of the frequency response away from $k_x = k_y = 0$ so that the positive and negative frequency terms are weighted differently by the lens MTF.

A special case of (3) (above) of significant practical importance may be obtained by placing only a field stop aperture in one arm, for example the upper arm, and a more complex mask in the lower arm of the interferometric system. Then, Equation 12 can be written:

$$I_{wafer}(x,y) = 1 + \sum_{k_x}\sum_{k_y} I_i(k_x',k_y')e^{i2\pi k_x'x}e^{i2\pi k_y'y} + 2\sqrt{\sum_{k_x}\sum_{k_y} I_i(k_x',k_y')e^{i2\pi k_x'x}e^{i2\pi k_y'y}}\cos(4\pi wx)$$

$$(17)\quad = 1 + \sum_{k_x}\sum_{k_y} I_i(k_x',k_y')e^{i2\pi k_x'x}e^{i2\pi k_y'y} + 2\sum_{k_x}\sum_{k_y} M_i(k_x,k_y)T_E(k_x,k_y)e^{i2\pi k_x'x}e^{i2\pi k_y'y}\cos(4\pi wx)$$

$$= 1 + \sum_{k_x}\sum_{k_y} I_i(k_x',k_y')e^{i2\pi k_x'x}e^{i2\pi k_y'y} + \sum_{k_x}\sum_{k_y} M_i(k_x,k_y)T_E(k_x,k_y)e^{i2\pi k_y'y}\left[e^{i2\pi(2w+k_x)x} + e^{-i2\pi(2w-k_x)x}\right]$$

Equation 17 was derived under the assumption that the field stop is sufficiently large that the Fourier components associated with M_u are at much smaller frequencies than those included in M_i. More particularly, each frequency in the summations in Equation 17 may be replaced by an appropriate function to restrict the pattern to the area defined by the field stop. That is:

$$e^{i2\pi k_x'x}e^{i2\pi k_y'y}$$

$$(18)\quad \rightarrow \iint e^{i2\pi k_x'x}e^{i2\pi k_y'y} ab\frac{\sin\left[2\pi(k_x'-k_x)a/2\right]}{\left[2\pi(k_x'-k_x)a/2\right]}\frac{\sin\left[2\pi(k_y'-k_y)b/2\right]}{\left[2\pi(k_y'-k_y)b/2\right]}T_E(k_x'-k_x,k_y'-k_y)dk_x'dk_y'$$

where a and b are the linear dimensions of the field stop and use has been made of the equivalence between multiplication and convolution in Fourier transform pairs.

This result still may not fully resolve the constraint issue noted in connection with Equation 16.

In particular, there are constraints on the Fourier coefficients, e. g., $Ml(k_x,k_y) = Ml^*(-k_x,-k_y)$, that are not consistent with an arbitrary final image. As noted above, this can

5   be avoided by shifting the optical system center frequency response away from $|k| = 0$. One possible optical scheme that accomplishes this is shown in **Figure 11**.

Referring now to **Figure 11**, effective masks 41 and 42 are employed, with mask 41 suitably comprising a simple open field stop aperture. A prism 71 is suitably disposed behind mask 42 to provide an angular offset of the frequency components. Center optical

10   rays 72 and 73 are shown to provide additional information. Prism 71 may be advantageously chosen such that zero frequency rate emerging from mask 42 is directed to the edge of the aperture of lens 33. In this configuration, prism 71 effectively imparts an overall tilt, or bias, w_{tilt}, to the frequency components accepted by the lens system. In the illustrated embodiment, the prism angles are selected to tilt the zero spatial frequency

15   ray emerging from mask 42 so that it just misses the aperture of the first lens (33). Specializing this result to a simple field stop aperture as the upper mask, and again in the approximation that the nonzero Fourier coefficients of this aperture are at much lower frequencies than those of the mask and can initially be neglected, the total field at the mask becomes

20   (19) $$E(x,y) = e^{-i2\pi w x} + \sum_{k_x}\sum_{k_y} M_u(k_x,k_y)T_E(k_x - w_{tilt},k_y)e^{i2\pi(k_x-w_{tilt}+w)x}e^{i2\pi k_y y}$$

and the intensity is

$$I(x,y) = |E(x,y)|^2 = 1 + \sum_{k_x}\sum_{k_y} M_l(k_x,k_y)T_E(k_x - w_{tilt},k_y)e^{i2\pi(k_x-w_{tilt}+2w)x}e^{i2\pi k_y y}$$

(20) $$+ \sum_{k_x}\sum_{k_y} M_l^*(k_x,k_y)T_E(k_x - w_{tilt},k_y)e^{-i2\pi(k_x-w_{tilt}+2w)x}e^{-i2\pi k_y y}$$

$$+ \sum_{k_x}\sum_{k_y}\left[\sum_{k_x}\sum_{k_y} M_l(k_x,k_y)T_E(k_x - w_{tilt},k_y)M_l^*(k_x',k_y')T_E(k_x' - w_{tilt},k_y')e^{i2\pi(k_x-k_x')x}e^{i2\pi(k_y-k_y')y}\right]$$

By adjusting w_{tilt} so that, for example, only positive k_x are accepted by the lens system, the final constraints on forming an arbitrary image are removed. It should be noted that

25   there are many possible variants to using the prism as illustrated in **Figure 11**. For example, the prism could be placed in front of the mask; it could be replaced by an

appropriate diffraction grating used either in transmission or in reflection; Fourier plane filters could be used (e. g., apertures at the focus of the first lens (33) in the optical system) to select only appropriate subsets of the mask transmission.

Calculations of patterns that can be generated using this idea are shown in **Figure 13**. The top panel on the left (labeled All freq.) shows the result of using all reasonably available interferometric exposures. This panel is included for comparison to show the best pattern yet obtained with a large number of exposures and is essentially the same as the top left panel of **Figure 4**. The middle left panel shows the results of a double exposure: an imaging interferometric exposure and an incoherently illuminated optical exposure. This middle left panel shows the result of combining a single imaging interferometric lithography (IIL) exposure, offset (biased) in the y- or vertical direction, using the arrangement of **Figure 11**, and a traditional incoherently illuminated optical exposure, both with modest lens NA of 0.4. In the example shown in the middle left panel, the imaging interferometric exposure may be advantageously biased, for example at a y-spatial frequency of 0.5 by prism 71 of **Figure 11**. In accordance with a preferred embodiment, this bias is then effectively canceled out by the interferometric optics (e.g., mirrors 45-48 of **Figure 7**) to ultimately yield the proper frequency distribution for the pattern. A mask with the desired pattern is suitably placed in one arm of the optical system, and an open aperture delineating the field is suitably placed in the other arm. For the example shown in **Figure 13**, the pattern is repetitive with a period $P_x = 12\,CD$ in the horizontal (x) direction and $P_y = 5\,CD$ in the vertical (y) direction. The Fourier series representation of the pattern has frequency components $k_{n,m} = 2p(nx/P_x + my/P_y)$. The corresponding spatial frequencies, normalized to the CD, are $CD/P_x = 0.083$ and $CD/P_y = 0.2$ and the current practically realizable maximum values of (n, m) supported by interferometric lithography are (11, 5), i. e., $n_{max} = \text{Int}(2P_xCD/\lambda1) = \text{Int}(P_x k_{ll})$, where the Int function returns the integer portion of the argument. The prism 71 was chosen to tilt all of the frequencies by $w_{till} = 0.5$. Therefore, the high spatial frequency Fourier components, e.g., m=3, 4 are shifted into the collection cone of the lens 33. The bias, w_{ll}, introduced by the interferometric optics, e.g., mirrors 45-48 in **Figure 7**, were chosen so that $2w_{ll} = w_{till}$ and the offset tilt just cancels the bias added by the interferometric optics.

With continued reference to **Figure 13**, the bottom left panel shows a similar calculation for a lens NA of 0.7. Interestingly, while the extreme left and right edges of the pattern are more filled out for the higher NA, the tab at the center of the bottom feature

is less well defined at the higher NA. This is largely because this feature requires higher spatial frequency components in the x-direction that are not optimally supplied by either the interferometric or the imaging optical exposure. This may be remedied in the top right panel which shows the results of two imaging interferometric exposures, one biased by

5   the same $w_{tilt} = 0.5$ in y and one biased by the same amount in x to provide the spatial frequencies necessary to more satisfactorily define this feature, along with an incoherently illuminated standard optical exposure, all at a lens NA of 0.4. Clearly, the tab is better defined for this exposure. The undulation of the horizontal bars results because the lower frequency components are not present in exactly the correct amplitude

10   and phase. These components arise from each of the imaging interferometric exposures (second term in Equation 19) as well as from the optical exposure. Since most realistic microelectronic patterns will inevitably have small features in both directions, two interferometric exposures are likely to be necessary. The middle right panel shows the result of substituting a single, low frequency interferometric exposure (at a frequency of

15   λ/P_x) in place of the traditional optical exposure. The result is very similar to the previous panel, but the exposure required is much simpler. Finally, the bottom right panel shows a calculation of the image for two imaging interferometric exposures using a $NA = 0.7$ lens along with a single interferometric exposure at λ/P_x. This result is almost comparable to the best possible pattern shown on the top left, but requires only three exposures and

20   is compatible with the full complexity of microelectronic processing. These examples serve to illustrate the flexibility permitted by the combination of imaging interferometric and traditional imaging exposures. There are many ways to get to the desired result.

Very importantly, imaging interferometric exposures are not restricted to periodic arrays of structures. This is clearly demonstrated by the earlier example of imaging the

25   non-repetitive field stop. Any arbitrary pattern can be described as a Fourier series, where the repetitive period is the exposure field. For typical ULSI scales, this means that there are a very large number of Fourier components that must be included (*e.g.*, potentially on the order of 100 million). Clearly, this is unrealistic if individual Fourier components are separately exposed; but is not a problem for imaging interferometric exposures which

30   combine the capabilities of imaging optics to deal with large numbers of frequency components and those of interferometry to allow high spatial frequencies.

There are several possibilities for optimization which may be further explored in the context of the present invention. For example, where the total exposure is divided

into several sub-exposures, it becomes a straightforward procedure to adjust the relative

intensities of these exposures. Further, the imaging interferometric exposures involve two

(or perhaps more) optical paths and again it is possible to adjust the intensities of the

optical beams in these paths. Additionally, as the last two panels discussed illustrate

5   (Figure 13), it is sometimes advantageous to adjust the lens *NA* between the various sub-

exposures. That is, the lens *NA* for the incoherent optical exposure could have been

reduced to the point that it only passed the single frequency component used in the simple

interferometric exposure. The two beam intensities in the interferometric exposures were

taken as equal, and the intensities of each exposure were also equal for all of the imaging

10   exposures. For the simple interferometric exposure (*i.e.*, just two beams only, field-stop

apertures in each arm), the intensity was adjusted to provide a very qualitative best fit to

the desired pattern.

It remains to specify a procedure for specifying and manufacturing the masks that

are needed to define an arbitrary image. Note that this is now a series of sub-masks since

15   different regions of frequency space require different sub-masks to form the complete

image. The total number of sub-masks is determined by, *inter alia*, the spatial frequency

content of the image, by the *NA*s of the optical systems used in the exposure. and by the

required image fidelity. The mathematics outlined above yields a functional design

apparatus. However, the complexity of real ULSI patterns makes this a difficult task. In

20   principle, the number of spatial frequencies to be reproduced may be as large as the

number of pixels in the image, which for a 2×3 cm^2 image and a CD of 0.18 mm may be

as large as 2×10^{10}!

Referring now to **Figure 12**, another approach is to use optics to produce the masks

from an original mask that completely defines the pattern. A complete pattern mask (81)

25   written by current mask making procedures, for example, electron-beam direct-write

patterning without any resolution enhancements such as serifs, helper bars, or phase

shifts, is illuminated by incoherent light. Behind the mask is a prism (82) that tilts the

exiting wavefronts, similar in function to the prism in **Figure 11**. This introduces a bias.

w_{bias}, in the spatial frequencies imaged by the optical system (lenses 33 and 34). The

30   intensity pattern at the wafer plane is given by:

(21) $$I(x,y) = \sum_{k_x}\sum_{k_y} I(k_x,k_y) MTF_{inc}(k_x - w_{bias}, k_y) e^{i2\pi(k_x - w_{bias})x} e^{i2\pi k_y y}$$

- 25 -

Instead of imaging the wafer, this intensity pattern can be used to expose a mask blank (83) which is subsequently developed and patterned to form a submask. This is precisely the submask that may be advantageously used in the arrangement of **Figure 11** to produce the required Fourier components at the wafer. It is straightforward to show

5 that satisfying the relationship,

(22) $2w = w_{bias}$

facilitates production of the proper spatial frequencies at the wafer plane.

—

CLAIMS:

1.   A two-dimensional spatial pattern in a photosensitive material on a substrate resulting from the process of:

a first exposure of said photosensitive material using a first optical arrangement including a first illumination system for providing illumination of a first mask characterized by a first mask pattern and a first imaging system for imaging said first mask pattern onto said photosensitive material on said substrate, said first exposure having a first intensity pattern;

a second exposure of said photosensitive material using a second optical arrangement, said second exposure having a second intensity pattern;

wherein each of said first and second intensity patterns provide a subset of the spatial frequencies necessary to define said two-dimensional spatial pattern;

combining said first and second intensity patterns to thereby define said two-dimensional spatial pattern in said photosensitive material; and,

processing said photosensitive material to instantiate said two-dimensional spatial pattern.

2. The process of claim 1 wherein said photosensitive material is a photoresist layer.

3. The process of claim 1 wherein said substrate is a wafer.

4. The process of claim 1 wherein said processing results in a physical change in said photosensitive material such that said photosensitive material acts as a mask for modifying appropriate properties of said substrate according to said two-dimensional spatial pattern.

5. The process of claim 1 wherein said second optical arrangement includes a second illumination system for providing illumination of a second mask characterized by a second mask pattern and a second imaging system for imaging said second mask pattern onto said photosensitive material on said substrate.

1   6. The process of claim 5 wherein said second optical arrangement further includes

2   a third illumination system for providing illumination of a third mask characterized by

3   a third mask pattern and a third imaging system for imaging said third mask pattern such

4   that the electric fields corresponding to said second mask pattern and said third mask

5   pattern coherently interfere to provide an intensity pattern on said photosensitive material

6   on said substrate.

        7. The process of claim 1 wherein said first and second exposure steps are performed sequentially in time.

        8. The process of claim 1 wherein said combining step includes the process of substantially simultaneously adding said first and second intensity patterns of said exposures using illumination sources with orthogonal polarizations.

        9. The process of claim 1 wherein said combining step includes the process of substantially simultaneously adding said first and second intensity patterns of said exposures using mutually incoherent laser illumination sources.

1   10. The process of claim 1 wherein said first exposure step includes the process

2   of exposing using an optical lithographic exposure system the lower spatial frequency

3   components of said two-dimensional spatial pattern to said photosensitive material,

4   wherein the magnitudes of the spatial frequencies of said lower spatial frequency

5   components are less than approximately NA_l/λ_l.

1   11. The process of claim 10 wherein said optical lithographic exposing step is

2   characterized by a wavelength band $(\sim\lambda_l)$, a numerical aperture NA_l, and a partial

3   coherence (σ_l), and said partial coherence is between the limits of $\sigma_l = 0$ (coherent) and

4   $\sigma_l = \infty$ (incoherent), said optical lithography exposing step providing a range of said

5   spatial frequencies extending to $< 2NA_1/\lambda_1$, with a modulation transfer function at each

6   of said spatial frequencies that depends on said σ_1 and on a pattern on a mask, said optical

7   lithography exposing step includes the process of:

8   illuminating, using said first optical illumination system, said mask; and

9   imaging said pattern on said mask, using said first imaging system, onto said

10   photoresist layer on said wafer.

1   12. The process of claim 1 wherein said second exposure includes the process of

2   exposing using multiple-beam interferometric exposures to provide the higher spatial

3   frequency components of said two-dimensional spatial pattern to said photosensitive

4   material, wherein the magnitudes of the spatial frequencies of said higher spatial

5   frequency components are greater than approximately NA_I/λ_I, wherein said second

6   exposure is characterized by:

7   an intensity pattern at said substrate with a spatial frequency established by the

8   angles of incidence of said multiple beams onto said photosensitive material on said

9   substrate,

10   an amplitude of said intensity pattern in said photosensitive material established by

11   an exposure dose used in said second exposure, and

12   a phase of said intensity pattern relative to a reference on said substrate.

1   13. The process of claim 1 wherein said second exposure includes the process of

2   exposing using imaging-interferometric exposures to provide the higher spatial frequency

3   components of said two-dimensional spatial pattern to said photosensitive material,

4   wherein the magnitudes of the spatial frequencies of said higher spatial frequency

5   components are greater than approximately NA_I/λ_I, wherein said second exposure is

6   characterized by

7   a central spatial frequency component at a central spatial frequency;

8   an amplitude of said central spatial frequency component established by an

9   exposure dose used in said second exposure;

10   a phase of said central spatial frequency component;

11   a range of said higher spatial frequency components with spatial frequencies within

12   a circle centered on said central spatial frequency having amplitudes and phases adjusted

13   so as to define said two-dimensional spatial pattern in said photosensitive material on

14   said substrate.

1   14. The process of claim 5 wherein said imaging-interferometric exposure is

2   created by a coherently illuminated imaging interferometric optical system comprising:

- 29 -

3   a coherent illumination source at a wavelength λ_2;

4   a second optical imaging system with numerical aperture NA_2 and magnification

5   M_2;

6   means for mounting said second mask at polar angles $(\text{arcsin}[M_2\sin(\theta_2)], \phi_2)$

7   relative to a coordinate system fixed to said second imaging optical system;

8   optical means for illuminating said second mask with substantially a uniform plane

9   wave at polar angles $(\text{arcsin}[2M_2\sin(\theta_2)], \phi_2)$ relative to said coordinate system;

10   means for mounting substrate at polar angles $(-\theta_2, \phi_2)$ relative to said coordinate

11   system;

12   optical means for directing a reference plane wave through a third mask to delimit

13   the areas of exposure on said wafer and imaging said third mask onto said wafer with the

14   zero-order spatial frequency of said imaging incident on said wafer at the polar angles $(-$

15    $\theta_2, \phi_2)$ relative to said coordinate system coherently with the optical fields resulting from

16   said illumination of said second mask and said second optical imaging system;

17   alignment means for adjusting wafer or relative path lengths of optical systems to

18   ensure proper phase relationship between frequency components of said first and said

19   second exposures;

20   resulting in said second exposure on said wafer characterized by:

21   two offset center spatial frequencies at $+2\sin(\theta_2)/\lambda_2$ and $-2\sin(\theta_2)/\lambda_2$ along the

22   direction described by ϕ_2;

23   spatial frequency components within circles in spatial frequency space centered at

24   each of said offset center spatial frequency of radius NA_2/λ_2; wherein relative amplitudes

25   and phases of spatial frequency components within said circles substantially reproduce

26   those of desired pattern on said wafer.

1   15. The process of claim 1 wherein said second exposure includes the process of

2   exposing, using imaging interferometric exposures created by a coherently illuminated

3   imaging interferometric optical system, to provide higher spatial frequencies to said

4   photoresist layer, wherein said high spatial frequencies are substantially above the spatial

5   frequency cut-off at about Na_1/λ_1 of the transfer function of said first exposure, wherein

6   said second exposure illumination and imaging systems are characterized by:

7   a coherent laser illumination source at a wavelength λ_2;

8   said second optical imaging system with numerical aperture NA_2 and magnification

9   M_2;

10   optical means for illuminating said second mask with substantially a uniform plane

11   wave at polar angles $(\arcsin[2M_2\sin(\theta_2)],\phi_2)$ relative to a coordinate system fixed to said

12   imaging optical system;

13   means for mounting said second mask at polar angles $(0,\phi_2)$ relative to said

14   coordinate system;

15   means for mounting wafer at polar angles $(0,\phi_2)$ relative to said

16   coordinate system;

17   optical means for directing a reference plane wave through a third mask

18   to delimit the areas of exposure on said wafer and imaging said third mask onto said

19   wafer with the zero-order spatial frequency of said imaging incident on said wafer at

20   the polar angles $(-\theta_2,\phi_2)$ coherently with the optical fields resulting from said

21   illumination of said second mask and said second optical imaging system;

22   alignment means for adjusting wafer or relative path lengths of optical

23   systems to ensure proper phase relationship between frequency components of said

24   first and said second exposures;

25   resulting in said second exposure on said wafer characterized by:

26   two offset center spatial frequencies at $+2\sin(\theta_2)/\lambda_2$ and $-2\sin(\theta_2)/\lambda_2$ along the

27   direction described by ϕ_2;

28   regions of spatial frequency space centered at each of said offset center spatial

29   frequencies of radius NA_2/λ_2; wherein relative amplitudes and phases of spatial

30   frequency components within said regions substantially reproduce those of desired

31   pattern on said wafer.

1   16. The process of claim 14 further includes the case wherein said second and

2   third masks are constructed such that the amplitudes and phases of the spatial

3   frequency components resulting from said illumination of said mask are substantially

4   the same as those desired in the final image within said regions of frequency space

5   without any constraints as to amplitudes and phases of the spatial frequency

6   components resulting in other regions of frequency space not collected by said optical

7   system.

1   17. The process of claim 14 further includes the case wherein said second and
2   third masks are constructed such that: the amplitudes and phases of the spatial
3   frequency components resulting from said illumination of said mask are substantially
4   the same as, but shifted in spatial frequency from, those desired in the final image and
5   said optical imaging system is adjusted such that said spatial frequencies print in the
6   desired regions of frequency space on said wafer. There being no constraint on the
7   spatial frequency components not within said regions of frequency space.

1   18. The process of claim 14 further includes the process of optically producing
2   said masks, using a complete mask and said coherently illuminated imaging
3   interferometric optical system, said optically producing step includes the process of:
4   imaging said desired regions of frequency space onto a blank, photoresist
5   coated, mask blank at least a portion of which is located in the wafer plane; and,
6   thereafter processing said mask blank to develop said photoresist and to transfer
7   said optically produced pattern to said mask.

    19. The process of claim 18 further includes the process of shifting said desired
region of frequency space to a different region from that needed for said desired
two-dimensional spatial pattern consistent with said optical imaging system.

1   20. The process of claim 9 further includes the process of:
2   aligning said offset center spatial frequency of said second exposure along the
3   x-frequency-axis to encompass high spatial frequencies engendered by small
4   structures with small dimensions along the corresponding x-spatial axis; and
5   aligning said offset center spatial frequency of said third exposure along the
6   orthogonal y-frequency-axis to encompass high spatial frequencies engendered by
7   small structures with small dimensions in the corresponding y-spatial axis to
8   maximize the spatial frequency coverage for rectilinear layout spatial patterns.

1   21. The process of claim 16 further includes the process of:
2   aligning said offset center spatial frequency of said second exposure along the
3   x-frequency-axis to encompass high spatial frequencies engendered by small
4   structures with small dimensions along the corresponding x-spatial axis; and

- 32 -

5   aligning said the center spatial frequency of said third exposure along the

6   orthogonal y-frequency-axis to encompass high spatial frequencies engendered by

7   small structures with small dimensions in the corresponding y-spatial axis to

8   maximize the spatial frequency coverage for rectilinear layout spatial patterns.

1   22. The process of claim 14 further includes the process of:

2   aligning said offset center spatial frequency of said second exposure along the

3   x-frequency-axis to encompass high spatial frequencies engendered by small

4   structures with small dimensions along the corresponding x-spatial axis; and

5   aligning said offset center spatial frequency of said third exposure along the

6   orthogonal y-frequency-axis to encompass high spatial frequencies engendered by

7   small structures with small dimensions in the corresponding y-spatial axis to

8   maximize the spatial frequency coverage for rectilinear layout spatial patterns.

1   23. The process of claim 18 further includes the process of:

2   aligning said offset center spatial frequency of said exposure to produce said

3   second exposure mask along the x-frequency-axis to encompass high spatial

4   frequencies engendered by small structures with small dimensions along the

5   corresponding x-spatial axis and

6   aligning said offset center spatial frequency of said exposure to produce said

7   third exposure mask along the orthogonal y-frequency-axis to encompass high spatial

8   frequencies engendered by small structures with small dimensions in the

9   corresponding y-spatial axis.

1   24. The process of claim 19 further includes the process of:

2   aligning said offset center spatial frequency of said exposure to produce said

3   second exposure mask along the x-frequency axis to encompass high spatial

4   frequencies engendered by small structures with small dimensions along the

5   corresponding x-spatial axis; and

6   aligning said offset center spatial frequency of said exposure to produce said

7   third exposure mask along the orthogonal y-frequency-axis to encompass high spatial

- 33 -

8   frequencies engendered by small structures with small dimensions in the

9   corresponding y-spatial axis .

25. The process of claim 1 wherein said first beam and said second beam are
derived from a single coherent radiation source.
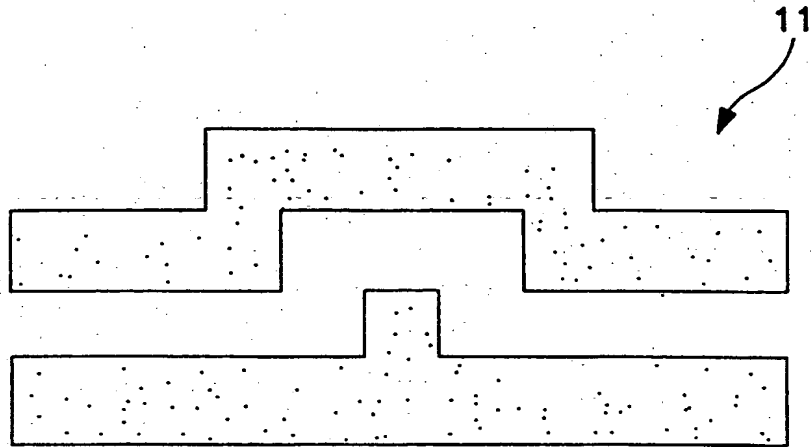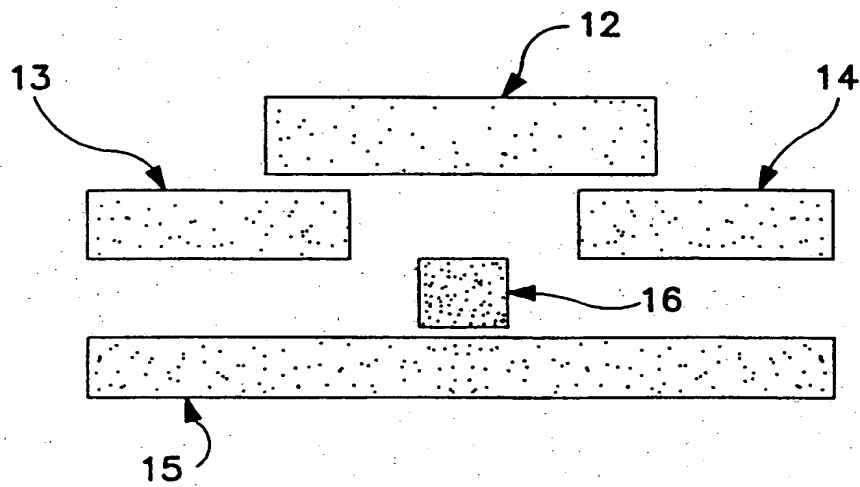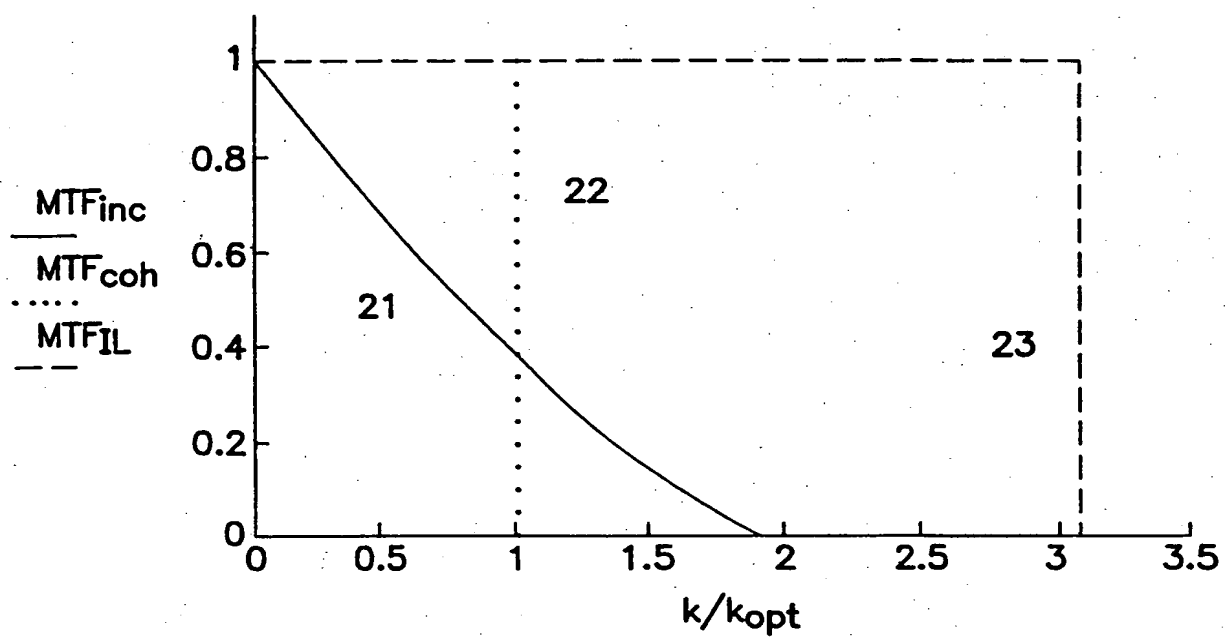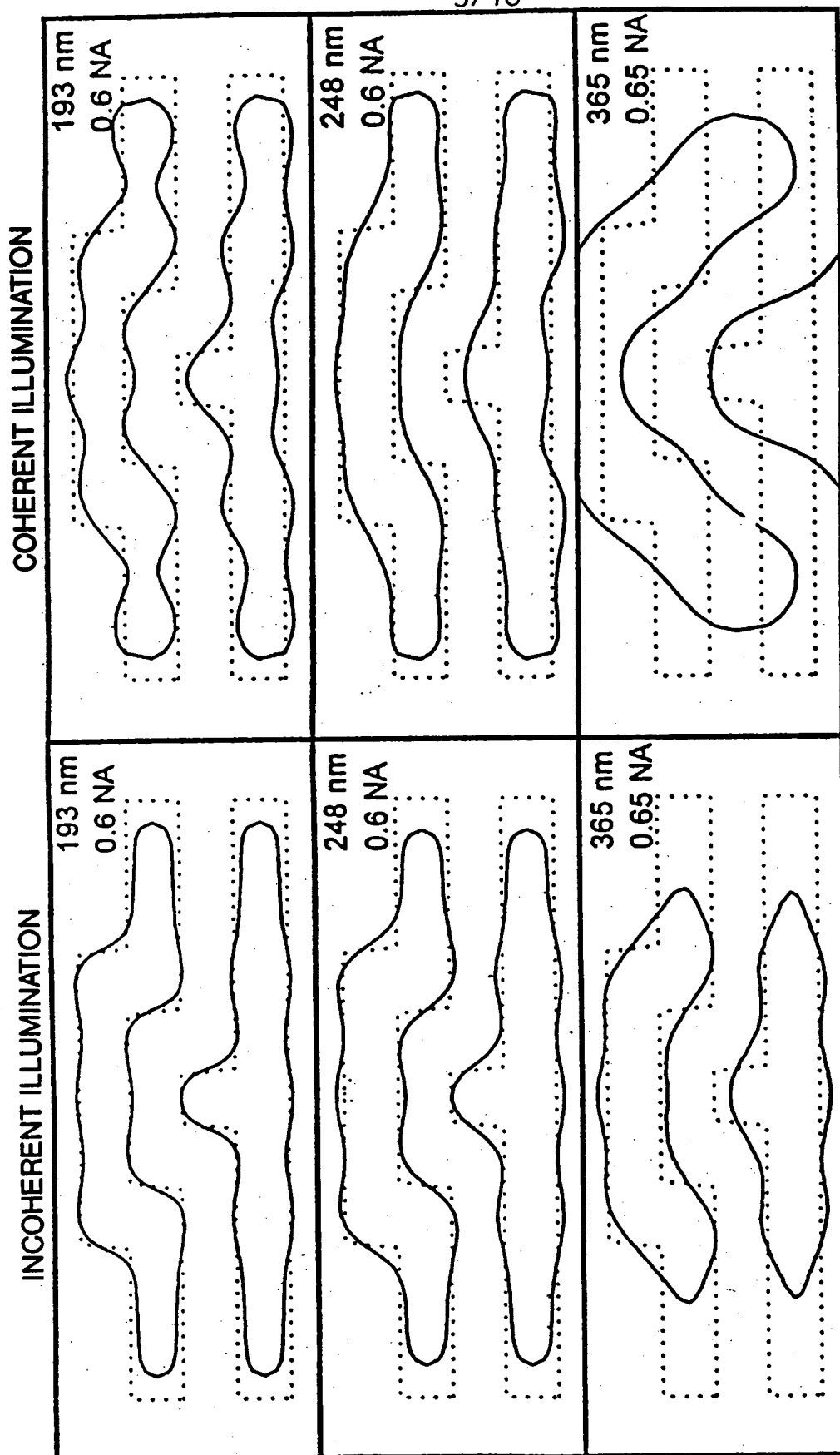
FIG. IA

FIG. IB

FIG. 2

FIG.3
PRIOR ART

Thres=0.05, N=10

Thres=0.08, N=6

Thres=0.12, N=5

$f_{min}=0, f_{max}=f_{iL},$
N=51

$f_{min}=f_{opt}, f_{max}=f_{iL},$
N=44

$f_{min}=f_{opt}, f_{max}=2f_{opt},$
N=18
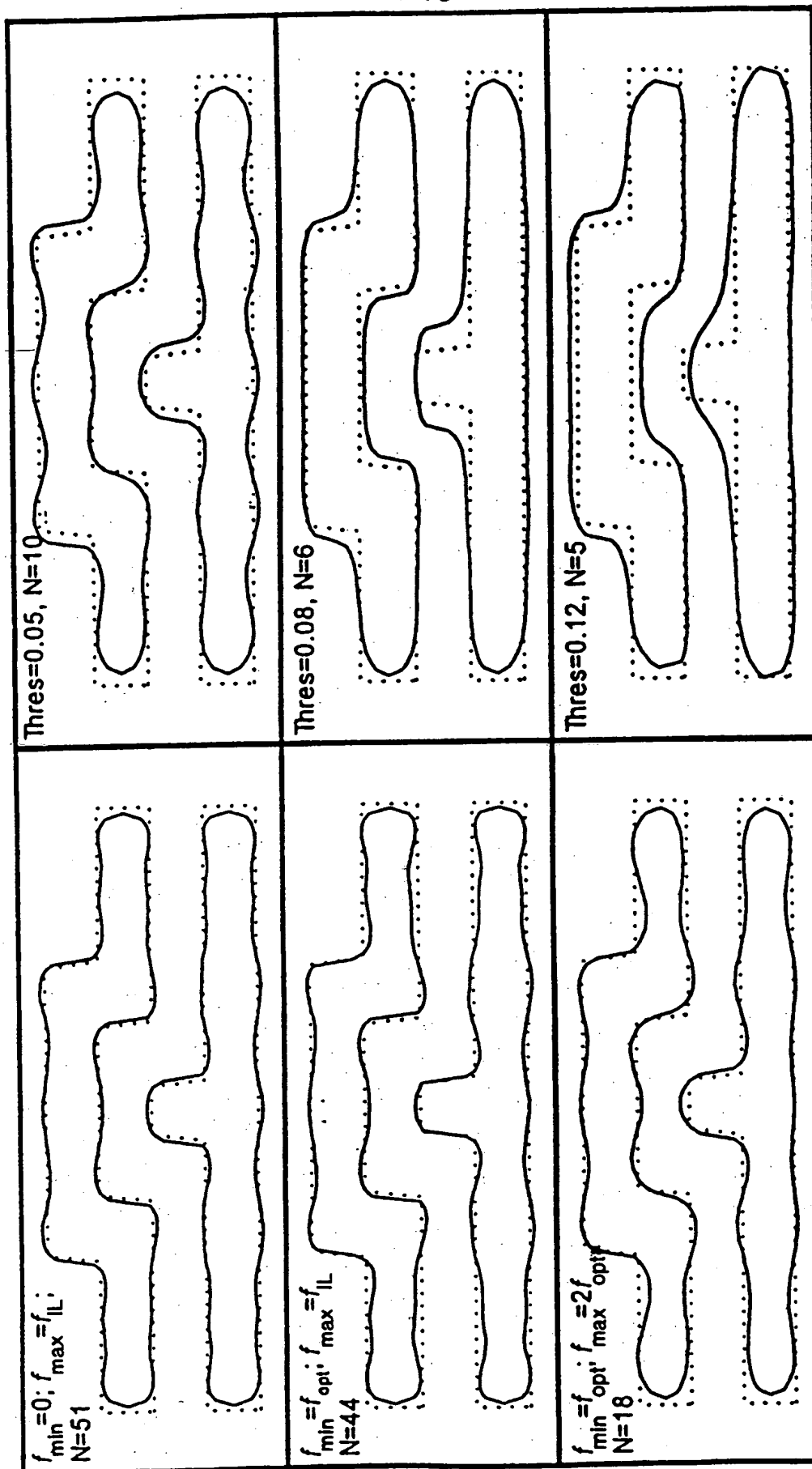
FIG. 4
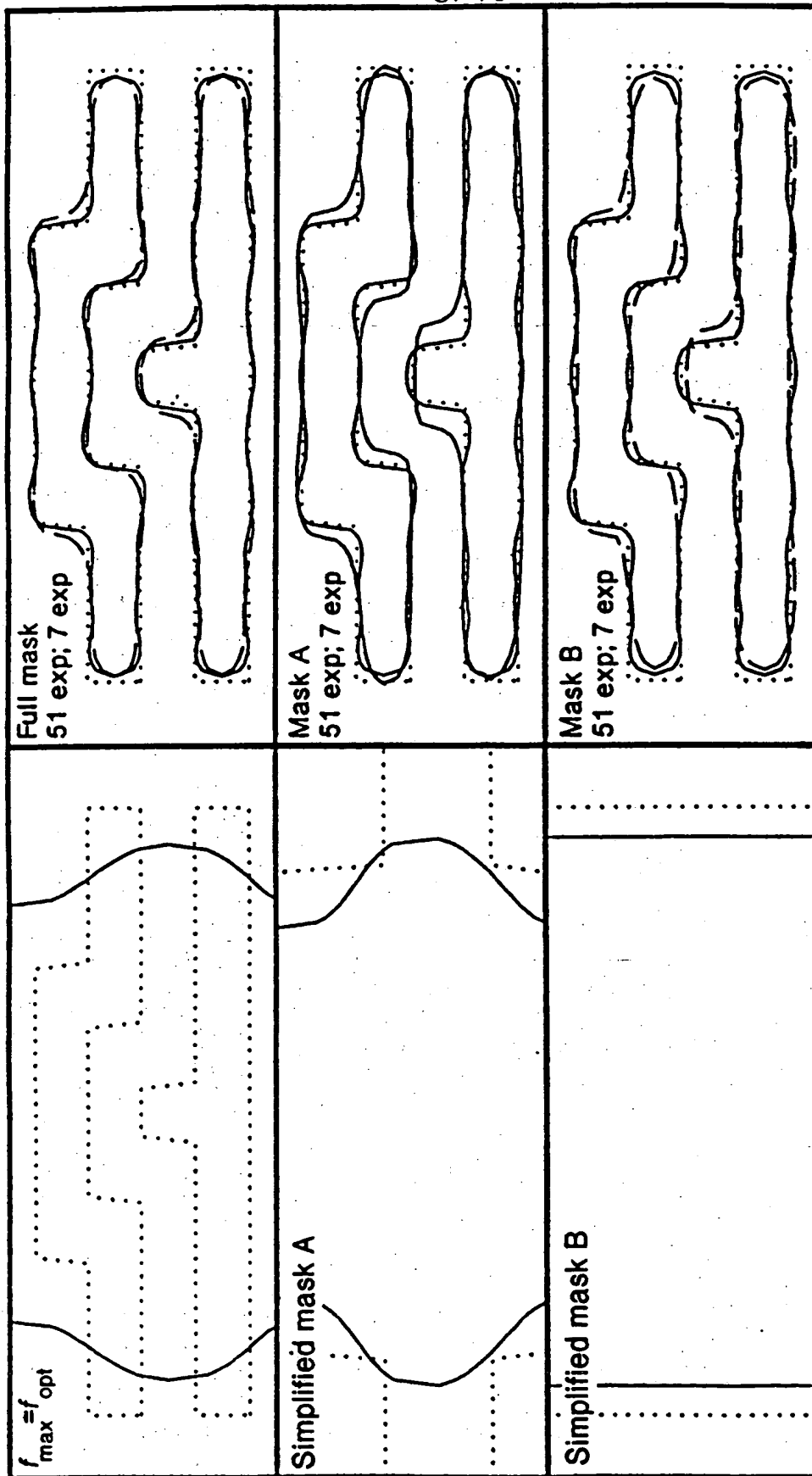
FIG.5
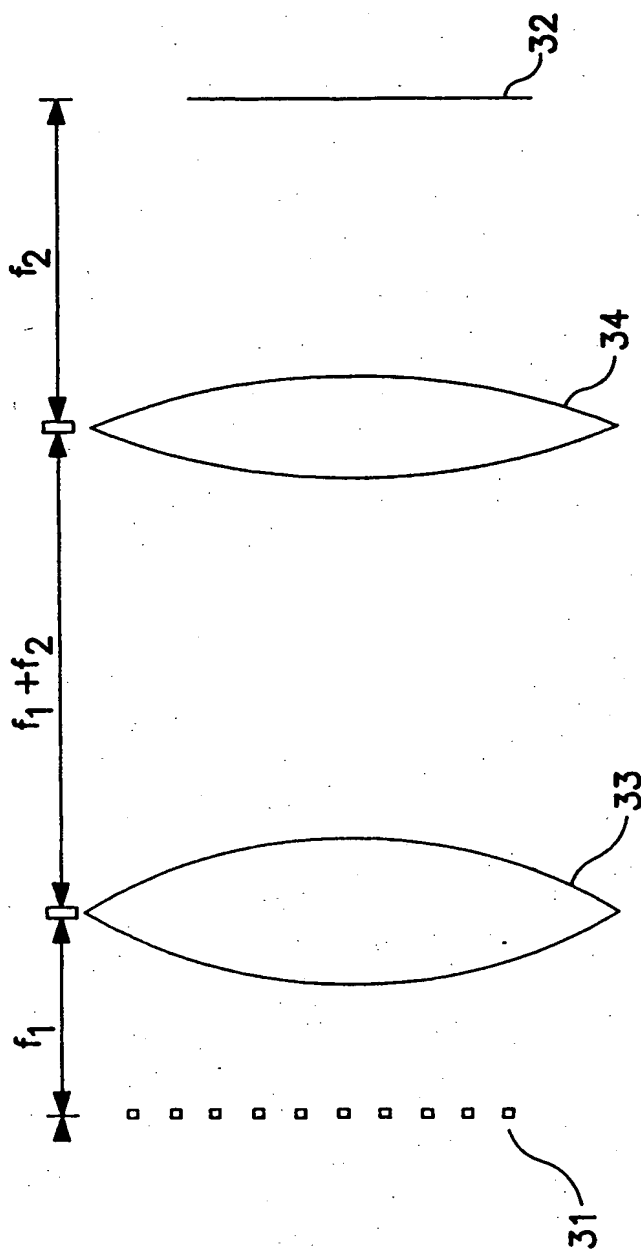
FIG. 6
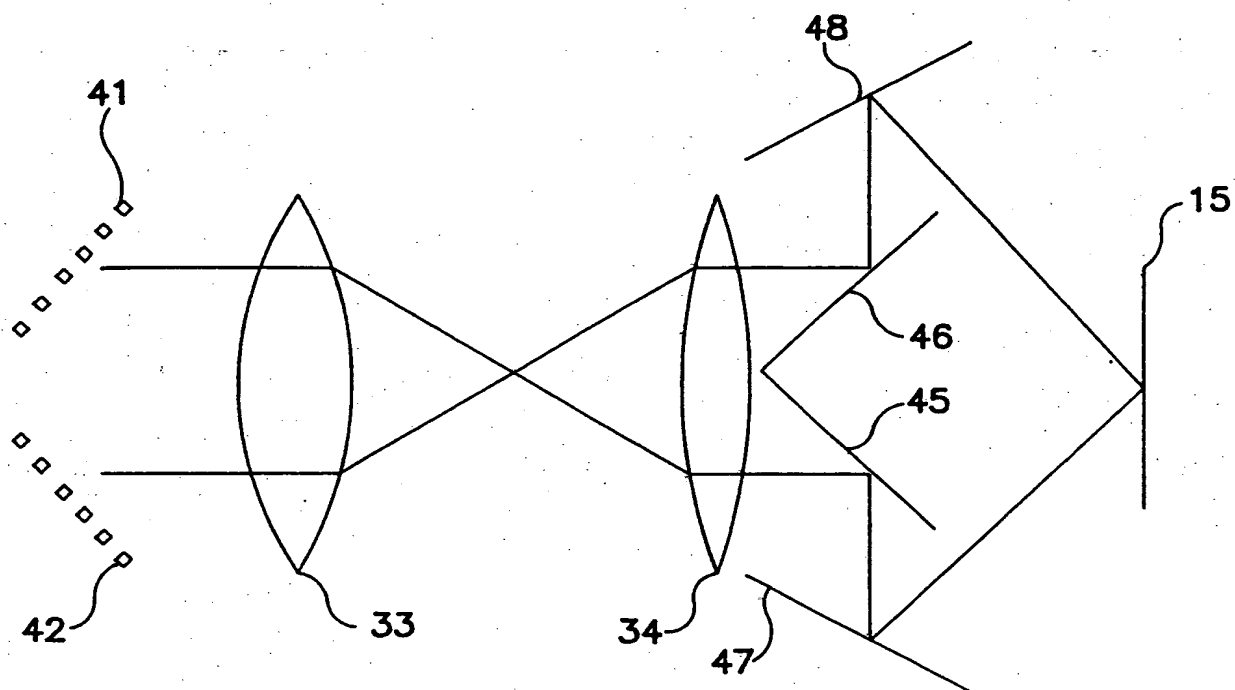
FIG. 7
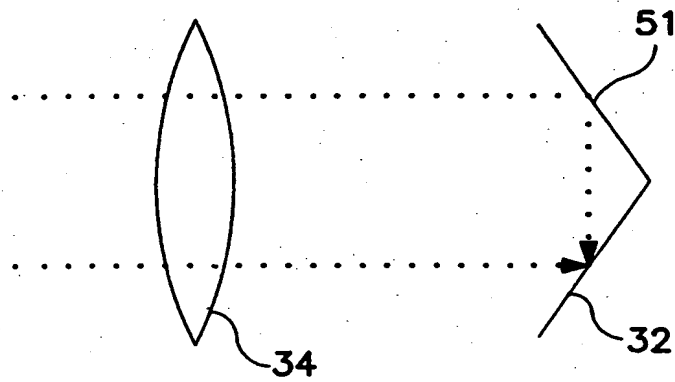
FIG. 8A
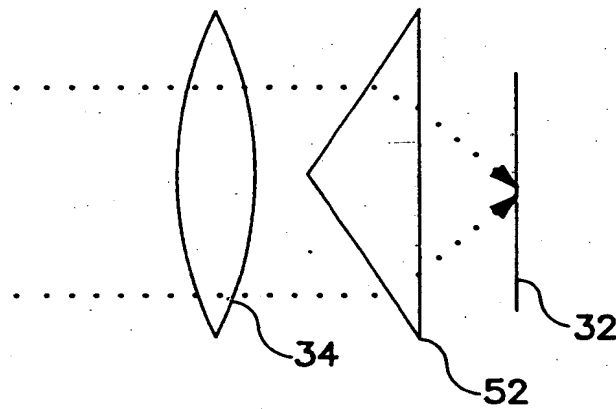
FIG. 8B
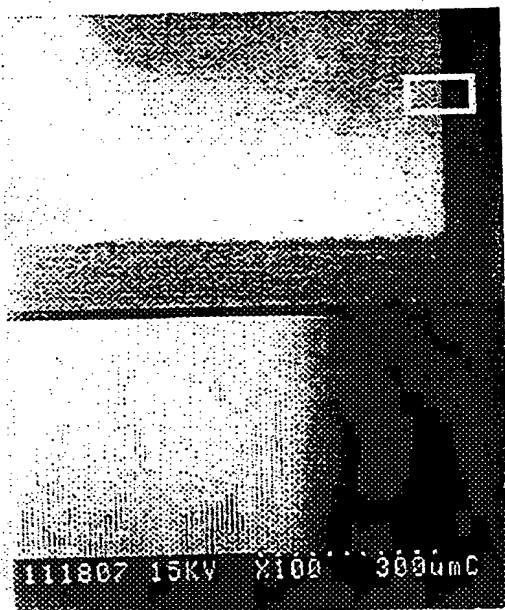
In-focus

FIG. 9A-1

In-focus
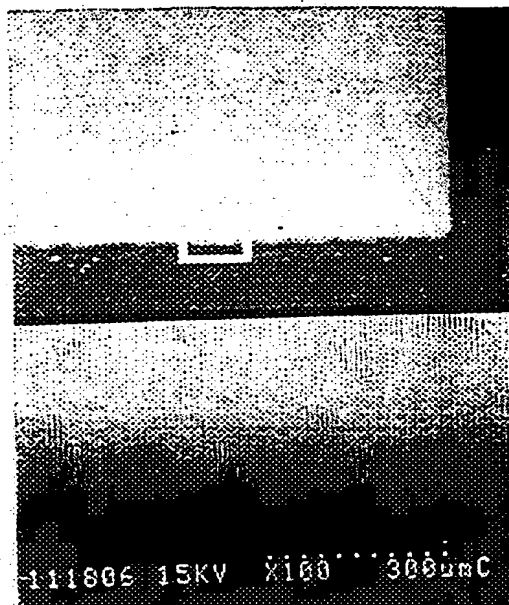
FIG. 9A-2

Out of focus
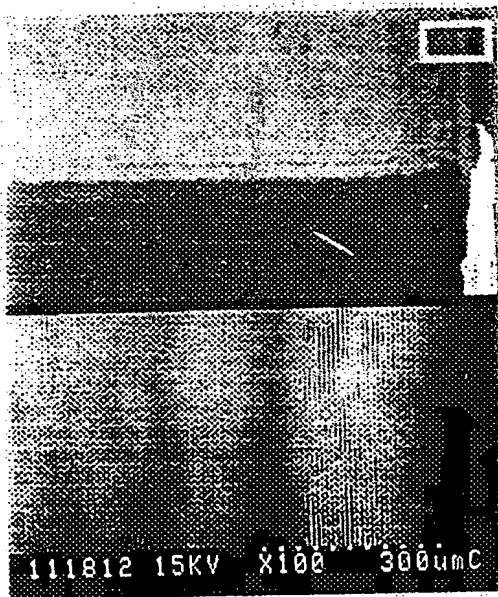
FIG. 9B-1

Out of focus
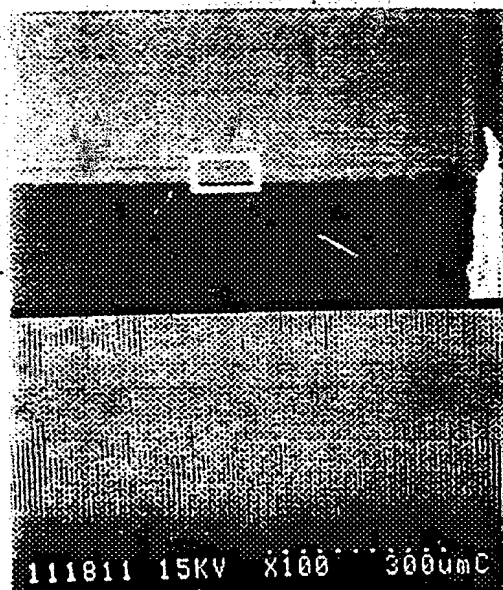
FIG. 9B-2
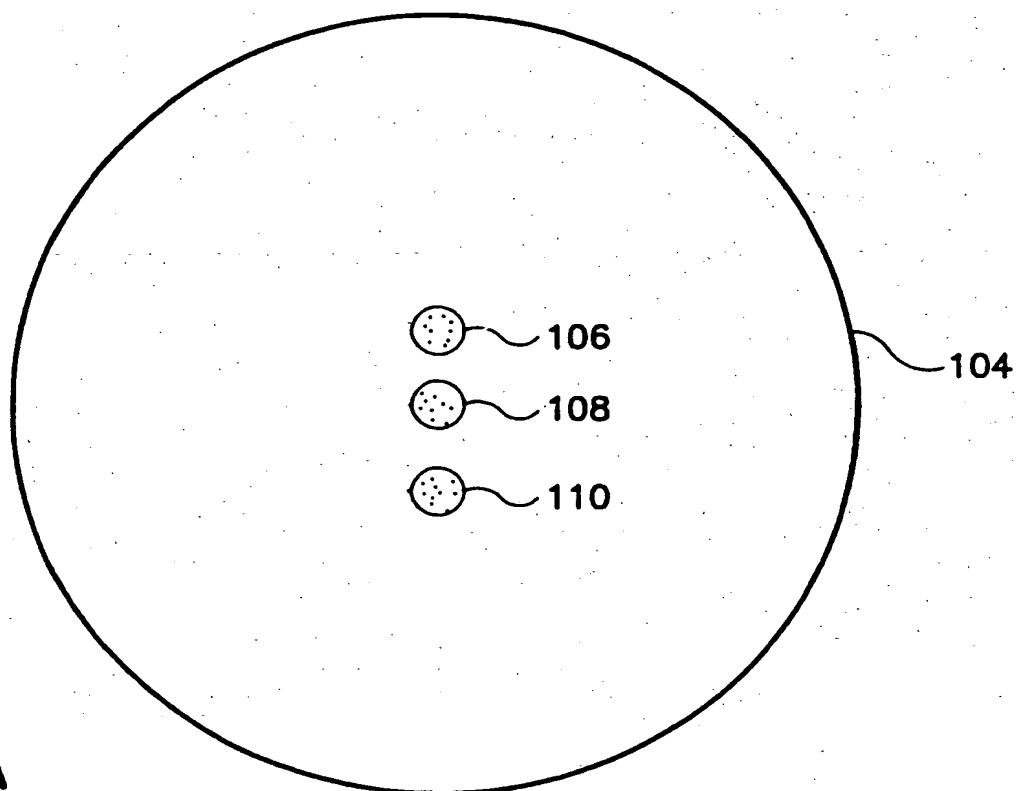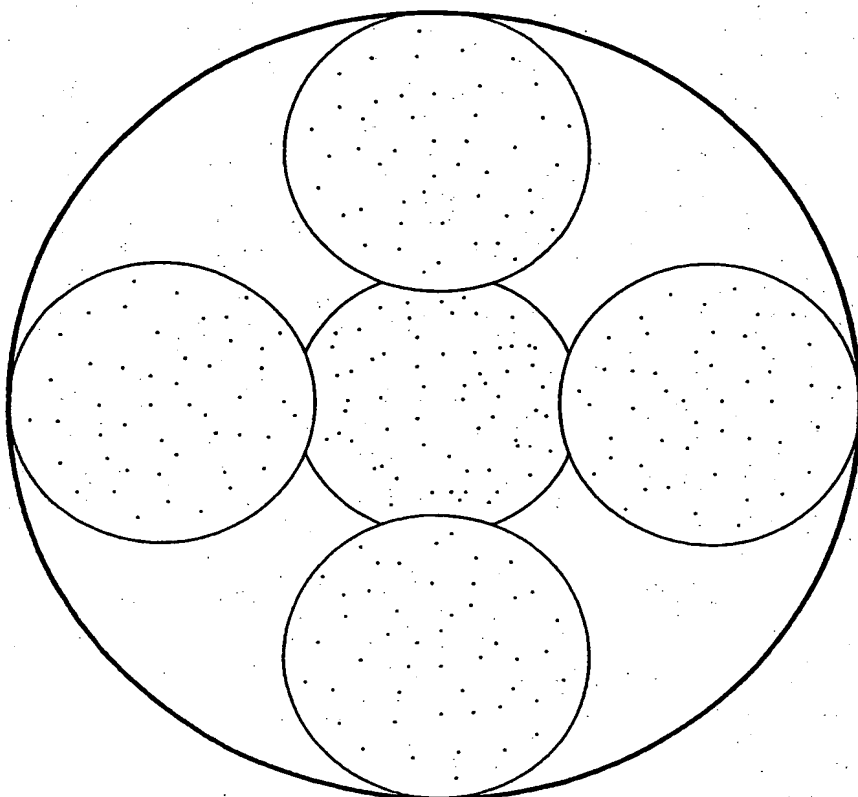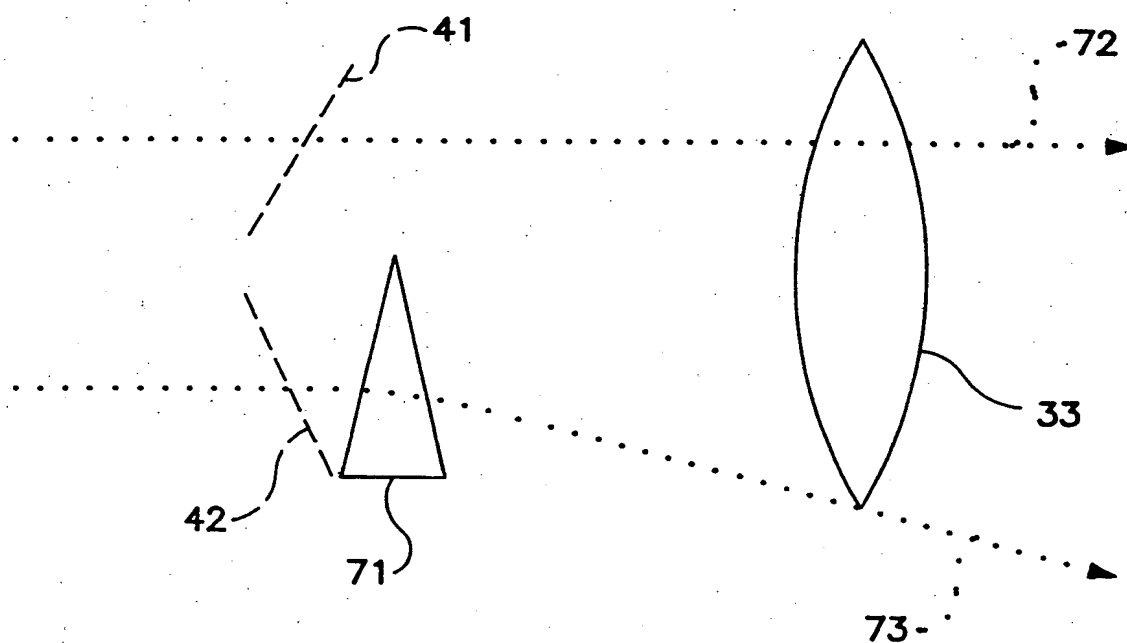
~106

~108

~110

~104

FIG. IOA

FIG. IOB

FIG. 11A

FIG. IIB

FIG. I2A

FIG. 12B

2054A1_I_>
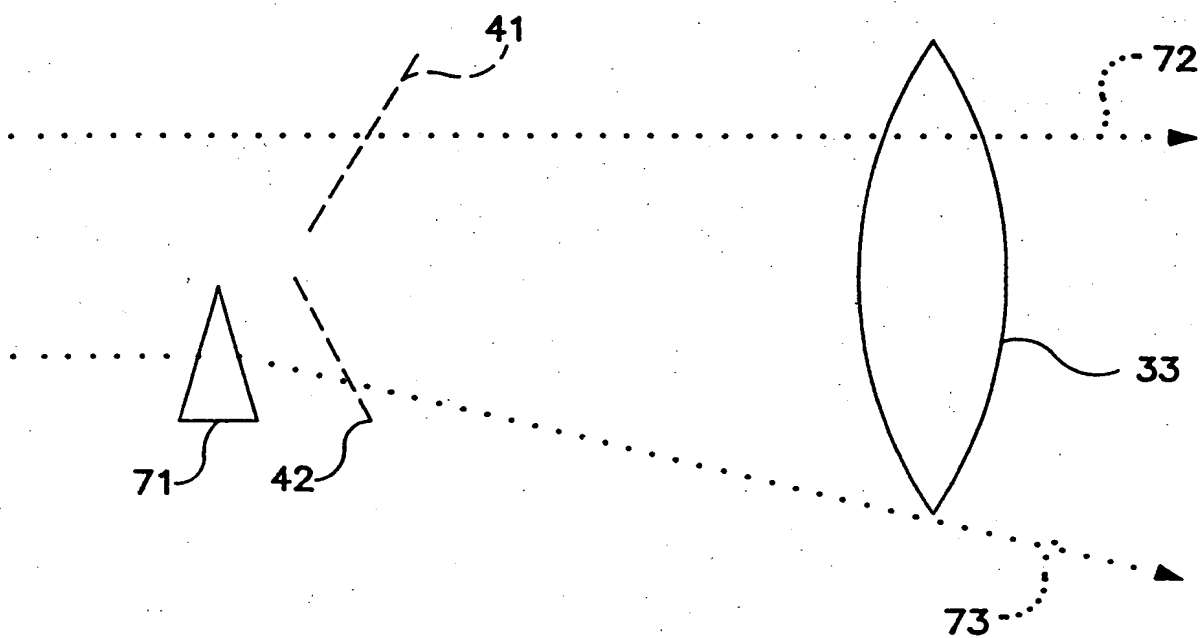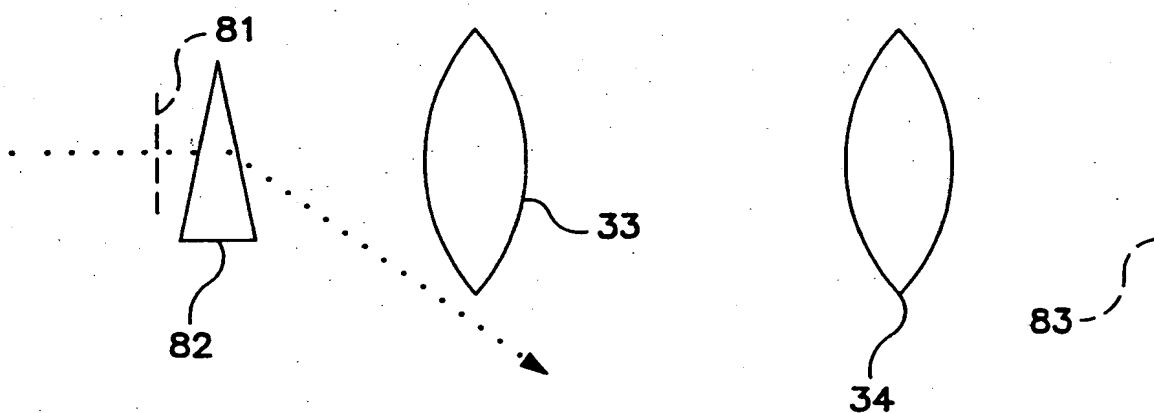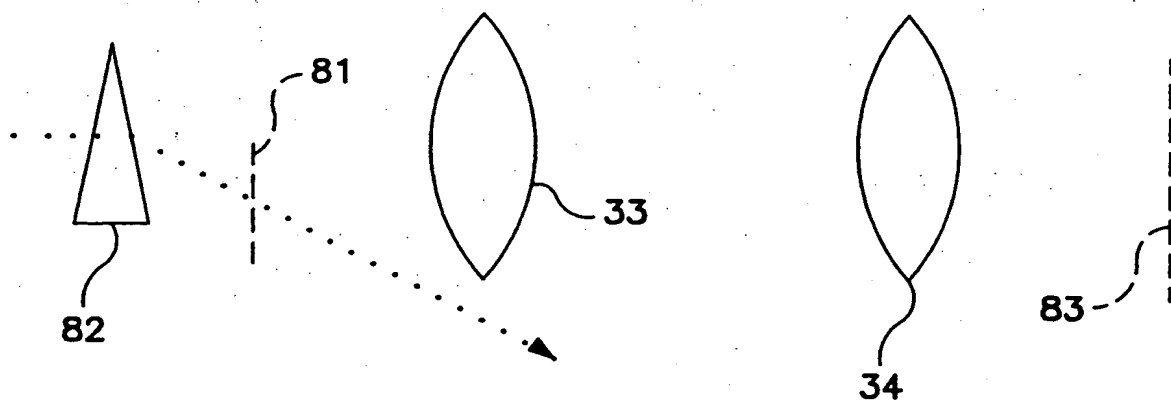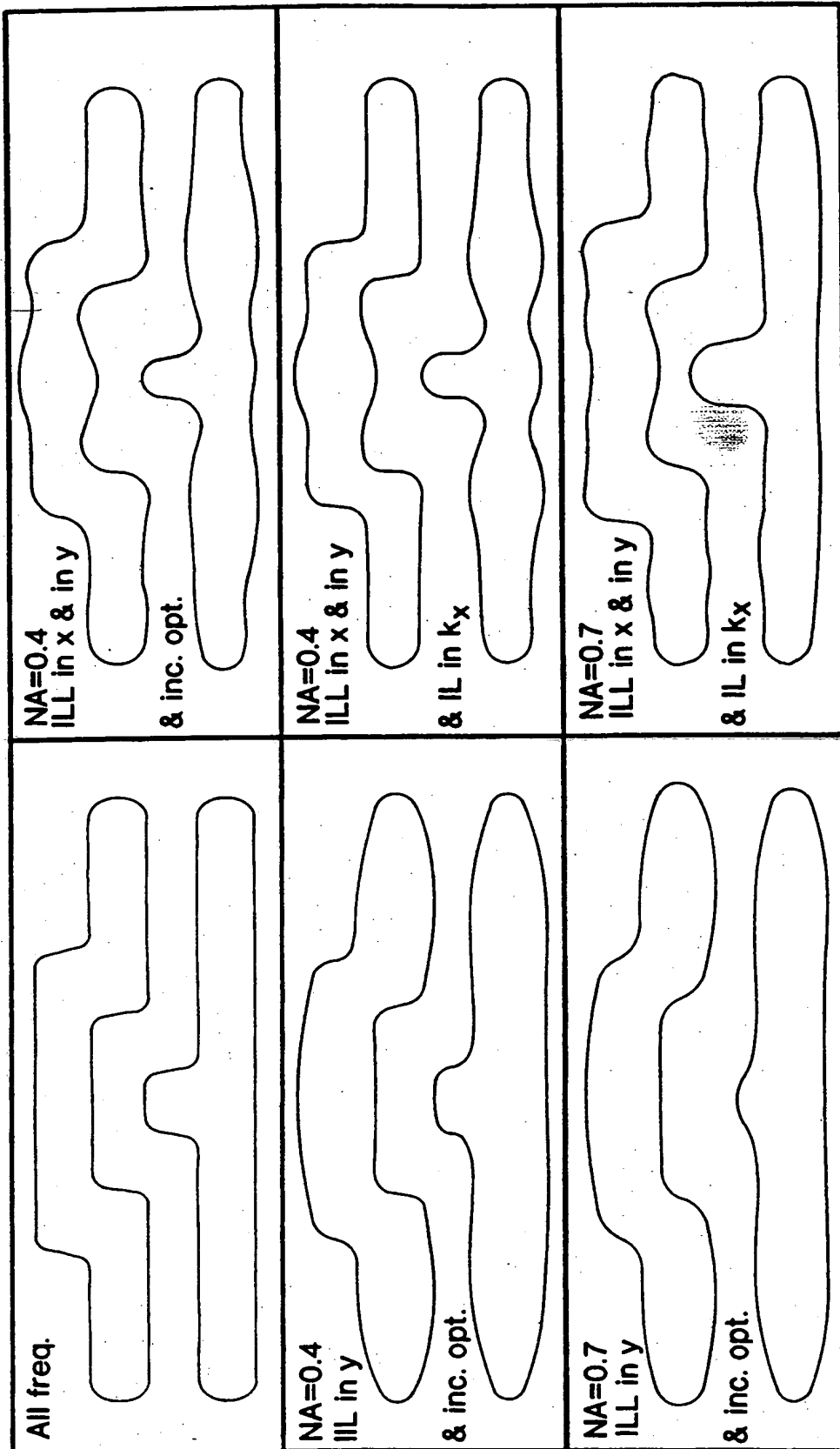
FIG.13
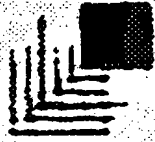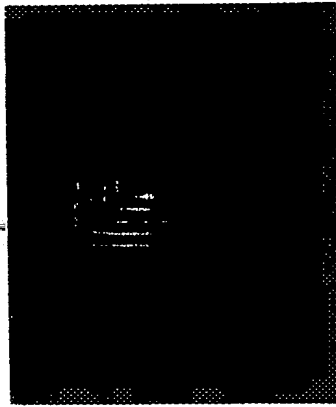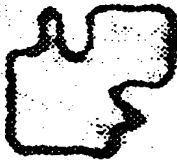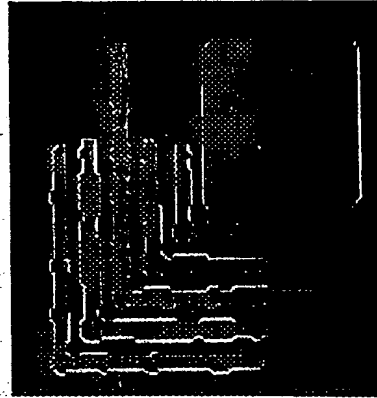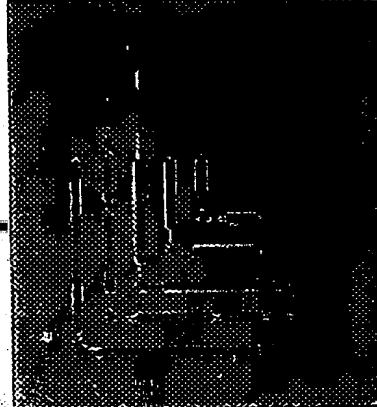
FIG.14E

FIG.14F

FIG.14C

FIG.14D

FIG.14A

FIG.14B
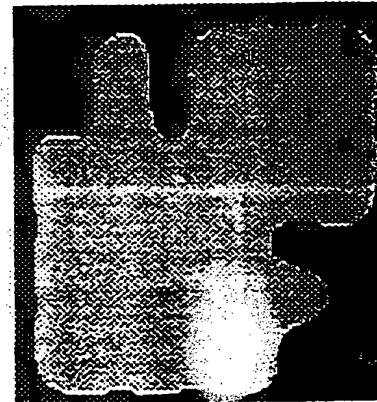
INTERNATIONAL SEARCH REPORT

A. CLASSIFICATION OF SUBJECT MATTER
IPC 6   G03F7/20

According to International Patent Classification(IPC) or to both national classification and IPC

B. FIELDS SEARCHED

Minimum documentation searched (classification system followed by classification symbols)
IPC 6   G03F

Documentation searched other than minimum documentation to the extent that such documents are included in the fields searched

Electronic data base consulted during the international search (name of data base and, where practical, search terms used)

C. DOCUMENTS CONSIDERED TO BE RELEVANT

Category °	Citation of document, with indication, where appropriate, of the relevant passages	Relevant to claim No.
X	WO 96 26468 A (UNIV NEW MEXICO ;BRUECK STEVEN R J (US); CHEN XIAOLAN (US); ZAIDI) 29 August 1996 cited in the application see page 12, line 3 - page 15, line 5 see figures 4-6,8-10	1-4,7, 10-13,25
X	US 5 415 835 A (BRUECK STEVEN R J ET AL) 16 May 1995 cited in the application see abstract see column 7, line 12 - line 42 see figure 21	1-4,7, 10-13,25

☐ Further documents are listed in the continuation of box C.   ☒ Patent family members are listed in annex.

° Special categories of cited documents :

"A" document defining the general state of the art which is not considered to be of particular relevance

"E" earlier document but published on or after the international filing date

"L" document which may throw doubts on priority claim(s) or which is cited to establish the publication date of another citation or other special reason (as specified)

"O" document referring to an oral disclosure, use, exhibition or other means

"P" document published prior to the international filing date but later than the priority date claimed

"T" later document published after the international filing date or priority date and not in conflict with the application but cited to understand the principle or theory underlying the invention

"X" document of particular relevance; the claimed invention cannot be considered novel or cannot be considered to involve an inventive step when the document is taken alone

"Y" document of particular relevance; the claimed invention cannot be considered to involve an inventive step when the document is combined with one or more other such documents, such combination being obvious to a person skilled in the art.

"&" document member of the same patent family

Date of the actual completion of the international search	Date of mailing of the international search report
3 June 1998	15/06/1998

Name and mailing address of the ISA	Authorized officer
European Patent Office, P.B. 5818 Patentlaan 2 NL - 2280 HV Rijswijk Tel. (+31-70) 340-2040, Tx. 31 651 epo nl, Fax: (+31-70) 340-3016	Heryet, C

Form PCT/ISA/210 (second sheet) (July 1992)

Patent document cited in search report		Publication date	Patent family member(s)		Publication date
WO 9626468	A	29-08-1996	AU	5298196 A	11-09-1996
US 5415835	A	16-05-1995	NONE		